TORSIONAL FATIGUE FAILURES

J. O. ALMEN

Research Laboratories Division, General Motors Corporation

Evaluation of the stresses and the fracture characteristics developed by torsional loads in parts made of metal. Torsional stress diagram is developed for the analysis of surface and sub-surface stresses. Evidence presented shows that the direct cause of fatigue failures from repeatedly applied torsional loads is always tensile stress; and the compressive stresses contribute only indirectly through altering the yield strength of the metal.

WHEN a twisting couple is applied to a uniform section specimen, such as a cylinder, every point on its surface is biaxially stressed. Tensile stresses act in the direction of 45 deg. helixes, and compressive stresses act in the direction of the opposite 45 deg. helixes. A third system of radial compressive stresses acts on sub-surface material. But the direct cause of fatigue failures from repeatedly applied torsional loads is always tensile stress, the compressive stresses contributing only indirectly through altering the yield strength of the metal.

The pattern of stresses in a specimen loaded in torsion is effectively shown in Fig. 1, in which it may be supposed that water is being pressed from a towel by the familiar process of wringing. In this analogy the stress acting in the direction of the woven stripes (left hand helix) is tension, and the stress acting perpendicular to the woven stripes (right hand helix) is compression. The radial compressive stresses are the result of tightening of successive layers on material beneath.

If the twisting couple is sufficiently increased, some of the threads that are loaded in tension will break and a tear will develop. The tear will, of course, extend in a direction normal to the tensile stress; that is, in the direction of a right hand helix. With continued growth the direction of the "crack" may change as the local direction of the applied force is altered by the extension of the tear. Because of the pronounced directional characteristics of the woven fabric, the twisted towel may not be acceptable as a specimen to demonstrate the nature of static failures in metals. It does, however, illustrate the orientation of the triaxial stresses and shows how static failures develop in this particular specimen.

Ductile Torsional Failures

When cylinders made of the usual metals of construction are statically loaded in torsion, the elastic surface stress pattern is the same as in the

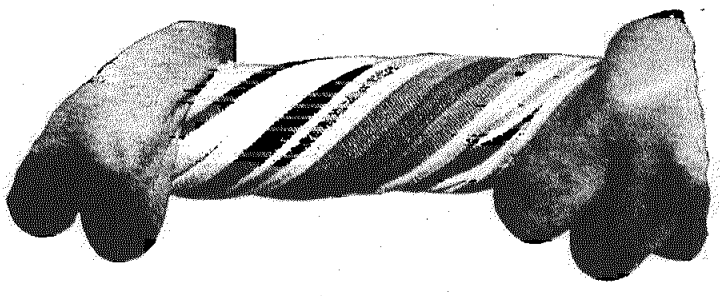

Fig. 1—Pattern of compressive and tensile stresses from torsional loading is illustrated by this analogy. Water is pressed from cloth by compressive forces acting perpendicular to the stripes. Cloth is torn by tensile forces acting in the direction of the stripes.

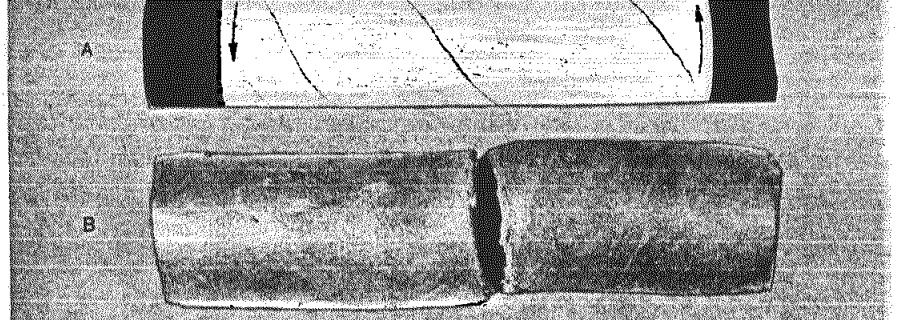

Fig. 2—Torsional Failures—(A) Brittle fracture from tensile stress in a sheet of specially selected paper glued to a rubber cylinder.—(B) Ductile failure from compressive and tensile yielding in a cylinder of modeling clay.

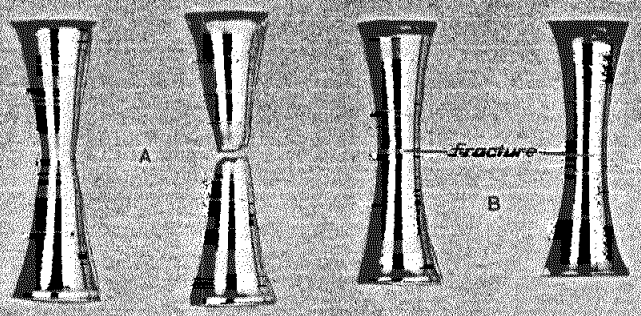

Fig. 3—Typical tensile stress fractures in specimens made of SAE 4340 of 32-36R$_c$ hardness.—(A) Necking and fracture due to static tensile loads.—(B) Fatigue fractures due to repetitive tensile loading.

towel but the characteristics of failure are not the same as noted in this simplified analogy.

Under static torsional loading of cylinders made from ductile materials, the fractures develop perpendicularly to the axis of the cylinder by transverse shear as is shown in Fig. 2 (*B*). This illustration shows a smooth cylinder of modeling clay that was twisted in the same direction as the towel shown in Fig. 1. It will be seen that the formation of the fracture was preceded by extensive plastic yielding. The tensile and compressive stresses contributed in substantially *equal* part to this plastic yielding, and failure occurred when the capacity of the material for plastic flow was exhausted. This is not difficult to visualize.

Since in static torsional tests of ductile materials the effect of the tensile stress component cannot be separated from the effect of the compressive stress component, it is convenient to treat them as a single new stress. A cylindrical bar statically loaded in torsion, therefore, is said to be stressed in transverse shear and longitudinal shear, each of which acts midway between the tensile and compressive stress components and 90 deg. to one another.

Brittle Fractures from Static Loads

When static torsional loads are applied to materials in which the effects of tensile and compressive stress components are *unequal*, the effects of the two components must be considered separately, because the characteristics of the resulting fracture will change from shear failure toward tensile failure as ductility is decreased.

In Fig. 2 (*A*) a rubber cylinder is shown on which is glued a sheet of specially selected paper. This paper is peculiar in that it has a minimum of directional properties; that is, its tear strength is substantially the same in any direction. A twisting couple of sufficient magnitude to tear the paper was applied to the rubber cylinder. Because of its low ductility, fractures occurred in the paper covering without visible evidence of plastic deformation; that is, the failures were brittle in character.

Since the rubber cylinder was twisted in the same direction as the towel, Fig. 1, the paper fractures are normal to the tensile stress components that caused the fractures. When the direction of the twisting couple is reversed, fractures in the paper covering the rubber cylinder will, of course, extend in the direction of a left hand helix.

Identical metal specimens that behave like ductile materials when fractured by a single load will behave like brittle materials when the fractures result from repeated loads. This phenomenon is true whether the specimens are loaded in torsion, in bending, or in tension, or by combinations of these.

This dual role is effectively demonstrated by the experiment recorded in Fig. 3. The two steel specimens at the left, Fig. 3 (*A*), have been subjected to static tensile loads of sufficient magnitude to cause plastic extension with the familiar reduction of area prior to fracture.

The two specimens at the right, Fig. 3 (*B*), also have been subjected to tensile loads. In these the calculated stress ranged from a minimum of 32,500 to a maximum of 150,000 psi. These loads were repeated a sufficient number of times on each specimen to develop the fatigue fractures shown in Fig. 3 (*B*). It will be seen that these fractures are brittle in character notwithstanding the fact that the specimens are identical in material, heat-treatment, dimensions, and workmanship with the two specimens shown in Fig. 3 (*A*), which necked severely.

In the foregoing demonstration tensile specimens are used, because their plastic deformations are more easily recognized than are the plastic deformations of equal or greater magnitudes that occur in metal cylinders loaded in torsion.

Fatigue Failures Are Brittle Failures

As was shown by the paper covered cylinder, Fig. 2 (*A*), brittle fractures develop from tensile stresses. Since torsional fatigue fractures, even in ductile metals, are "brittle" fractures, they also develop only from the tensile component of torsional loads. It is therefore necessary to abandon the shear stress convention when dealing with fatigue and other forms of failure in which, because of the manner of loading or because the materials are inherently brittle, fractures occur without appreciable ductility. Unless the shear stress convention is abandoned, one cannot understand the mechanism by which residual stresses increase or decrease fatigue or brittle static strengths, nor

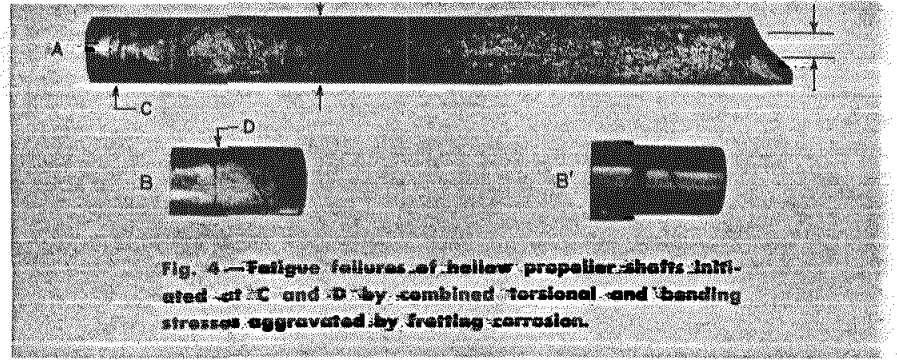

Fig. 4—Fatigue failures of hollow propeller shafts initiated at C and D by combined torsional and bending stresses aggravated by fretting corrosion.

can pre-stressing processes be applied to the best advantage.

The direction of torsional fatigue fractures will sometimes appear to deviate from a perpendicular to the principal applied tensile stress but, in the absence of seams or other major defects, deviations can usually be traced to residual stresses, surface stress raisers, or alterations in the stress pattern after a fatigue crack has begun to form.

Deviations from the latter cause sometimes occur in torsional specimens failing after relatively few stress cycles because the test stress is great and because, under repeated loads, plastic yielding occurs at stresses less than the static elastic limit. The extent of plastic yielding under repeated unidirectional loads varies with the magnitude of the dynamic stress and the duration of the load. Fractures in ductile fatigue specimens tested at high stress levels, therefore, may approach the characteristics of static torsional fractures.

In sound cylindrical torsional specimens free from residual stresses and severe stress raisers, tested by unidirectional load of such magnitude that failures occur after large numbers of stress cycles, the initial cracks are normal to the tensile stress components; that is, they extend in a direction approximately 45 deg. to the cylinder axis as occurred in the paper covered cylinder.

Fatigue Failures of Tubular Shafts

Portions of two marine propeller shafts 5.5 in. outside dia., which have centrally located longitudinal holes of 2.25 in. dia. are shown in Figs. 4(*A*), (*B*), and (*B*¹). Both shafts (not from the same boat) failed in normal service from fatigue fractures originating in fretted areas on the shafts. Fretting resulted from small amplitude rubbing of "pressed-on" bearing sleeves near the left (propeller) end of the shafts is shown by Fig. 4 (*B*¹), in which an artist has replaced the bearing sleeve that is missing in Fig. 4 (*B*). Minute relative motion between the bearing sleeves and the shafts in regions exposed to water caused deep pits, which formed a ring of severe stress raisers.

The combination of severe stress raisers, torsional propeller load, and superimposed bending stresses from off-center thrust of the propellers locally altered the direction of the principal tensile stress, as is indicated by the direction of the initial fractures at the left end of Figs. 4 (*A*) and (*B*). As the cracks progressed away from the fretted areas toward the right, their directions changed to approach normals to the directions of the torsional tensile stress, that is, they approach 45 deg helixes.

Since the shafts were tubular, and since the cracks progressed slowly, catastrophic failures did not develop immediately but long helical cracks formed instead.

Fractures Show Direction of Load

Note that the crack in Fig 4 (*A*) forms a left hand helix and that the crack in Fig. 4 (*B*) forms a right hand helix. Since torsional fatigue failures result only from the principal tensile stress, the direction of torsional loads causing fractures may be deduced by observing the direction of the fractures. It is thus apparent that the shaft of Fig. 4 (*A*) was loaded counter-clockwise as viewed from its ends, and that the shaft of Fig. 4 (*B*) was loaded in a clockwise direction. These deduced directions of loading were later verified from service records of the two shafts.

Coil Springs

Probably the most numerous of torsionally loaded machine elements are the familiar coil springs. The stress in the wire or bar from which coil springs are made is torsional whether the load is applied to extend or to compact the coils. The specimens *A* and *B* shown in Fig. 5 are one coil each of a conventional coil spring, which differ only in the direction of the applied load.

Specimen *A* is loaded in the direction to compress the coil as shown by the vertical load arrows. Under this load, the bar is twisted opposite to the twisting load that was applied to the towel, Fig. 1, and to the paper covered rubber cylinder, Fig. 2 (*A*). The tensile stress, therefore, is acting in the direction of a right hand helix as indicated by the stress arrows on the inner surface of the coil.

A fatigue fracture resulting from compacting loads on this spring would extend perpendicular to the tensile stress component in the direction of a left hand helix. As has been shown by Wahl (Ref. 1), the fracture would originate on the inner surface of the coil because of the greater stress in this region.

Specimen *B* is loaded in the direction to extend the coil. The tensile stress in this coil acts in the direction of a left hand helix and

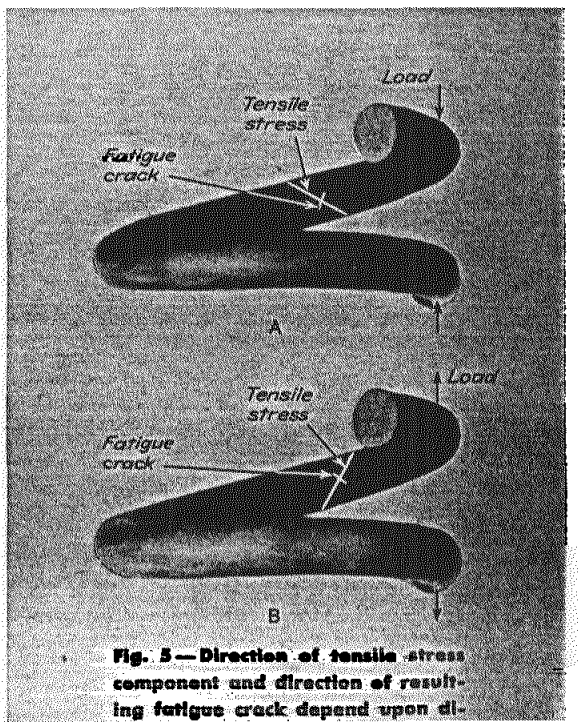

Fig. 5—Direction of tensile stress component and direction of resulting fatigue crack depend upon di-

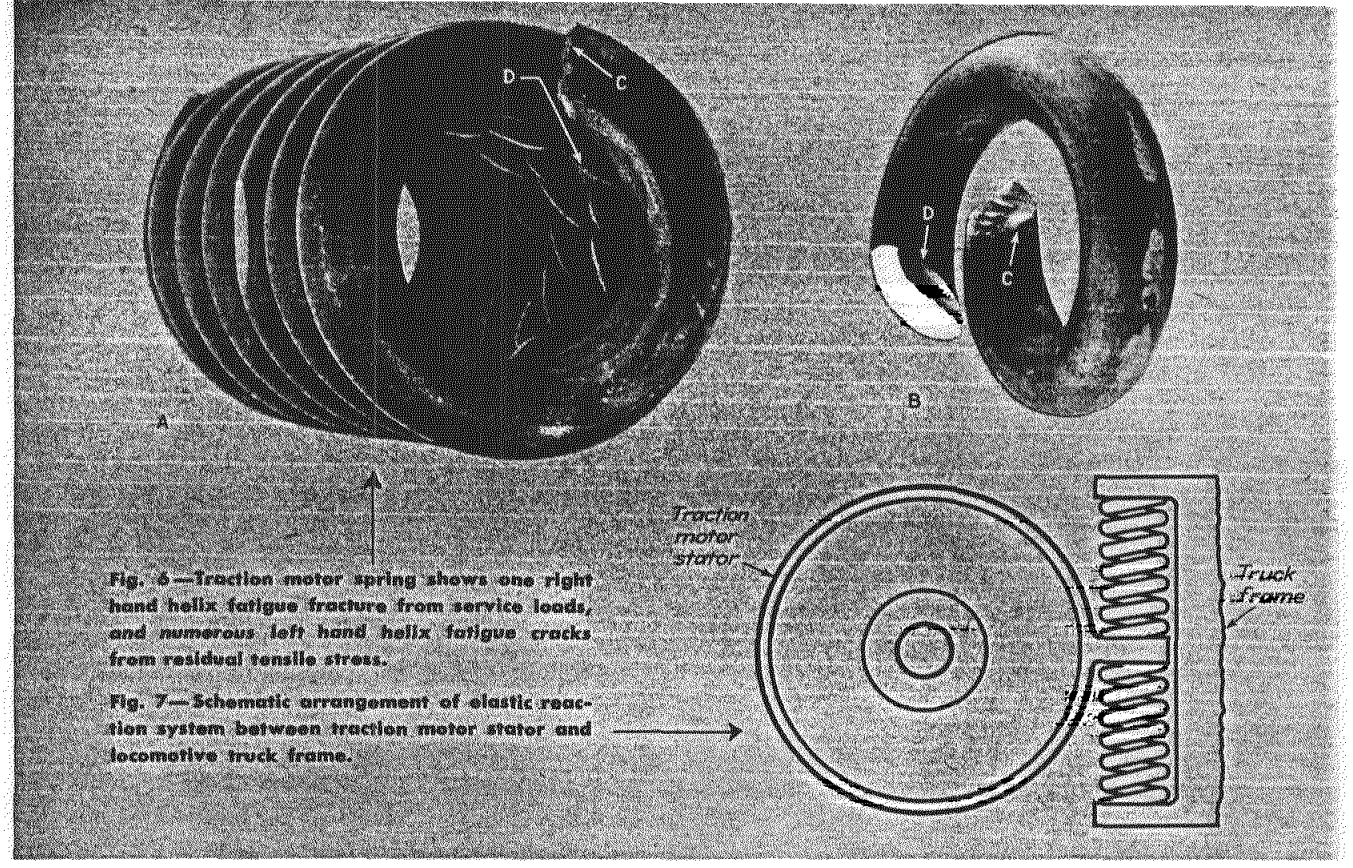

Fig. 6—Traction motor spring shows one right hand helix fatigue fracture from service loads, and numerous left hand helix fatigue cracks from residual tensile stress.

Fig. 7—Schematic arrangement of elastic reaction system between traction motor stator and locomotive truck frame.

any resulting fracture will develop in the direction of a right hand helix.

It follows that the direction of the load applied to a coil spring that has failed by fatigue can also be deduced by observing the direction of the fracture near its point of origin in relation to the direction of coiling. Note, for example, that the spring coils shown in Fig. 5 are wound as in left hand screw threads. Had they been formed as right hand screw threads, the directions of the tensile stress and therefore the directions of the fractures would have been reversed for the same directions of applied loads.

The ability to deduce the direction of the loads by observing the direction of fatigue fractures is often invaluable in discovering the cause or causes of failure, and in specifying materials and processing operations to prevent the recurrence of such failures.

Failures from Residual Stresses

The coil spring shown in Fig. 6 was part of the elastic reaction system between the traction motor stator and the truck frame of a diesel-electric locomotive. It was made from a hot rolled bar of AISI-1095 steel 18/16 in. nominal dia, which was hot wound in six coils having outer diameters of 3½ in. and inner diameters of 1⅞ in., heat-treated to a hardness of Rockwell C 45-47. Its purpose was to prevent the transmission of shock loads that result from rapid and violent changes in motor torque. A schematic sketch of the system is shown in Fig. 7, from which it is seen that the springs could be loaded only in the direction to compact the coils.

In Fig. 6 (*A*) is shown one complete fatigue fracture at *C*, originating on the inner diameter of the tapered end coil where the stress was locally aggravated by a severe stress raiser. Numerous non-fatal fatigue cracks as at *D* are also shown, which are made visible by magnetic particles as white diagonal lines on the inner diameters of most of the coils. More than 20 cracks, none of which developed to complete failure, could be counted in less than one-fifth of the total length of the coils.

In order that the characteristics of cracks and fractures could be more easily inspected, one coil was removed by grinding from the outer surface near the crack *D* as shown in Fig 6 (*B*). The complete fracture at *C* extends in the direction of a right hand helix originating in a sharp notch, apparently caused by the grip by which the bar was held during coiling; whereas each of the numerous cracks such as at *D* extend in the direction of left hand helixes, and have the origins in smooth surface metal.

Referring now to Fig. 5, and taking into account that these coils are wound in the opposite direction to the coils in the spring, Fig. 6, it is seen that the complete fracture at *C* is normal, being caused by the tensile stress component of the applied load.

Abnormal Fatigue Cracks

The multiplicity of cracks as at *D* are however abnormal because:
(a) *They appear to have been* caused by the compressive stress component of the applied load, and
(b) Many large cracks were formed but none propagated through the bar to complete failure.

Since fatigue cracks cannot develop from compressive stresses, the numerous cracks must have been caused by tensile stresses such as would result from extending the coils. It was not possible, however, to apply extension loads to this spring through the mechanism of the elastic system shown in Fig. 7. It was, therefore, tentatively assumed that the cracks were caused by the following:
(c) Rebound inertia loads extend-

ing the spring upon sudden reversal of torque, or

(d) Tensile components of residual stresses that were induced during processing, or

(e) A combination of the rebound inertia loads and tensile components of stresses induced during processing, (c) and (d).

Through correspondence with the manufacturer, it was learned that these springs were processed in such manner as to develop residual tensile stress normal to the direction of the fatigue cracks. The stress was developed by repeatedly overloading the springs in the direction of normal service loads sufficiently to develop permanant set. This process is extensively used by spring makers and is variously known as pre-setting, prestressing, bulldozing, and scragging. As applied to the spring shown in Fig. 6, the overloading produced a permanent set of 3/16 in. in its free height.

Further discussions of the abnormal fatigue cracks in the spring, Fig. 6, will be deferred until a diagram capable of representing their causes is described.

Torsional Stress Diagrams

The two conventions now used to represent torsional stresses are not suitable for torsional fatigue studies because:

(a) The strain rosette indicates only surface strain without regard to sign, and

(b) Section diagrams show only transverse shear.

For torsional fatigue studies, it is necessary to use a diagram that is capable of showing separately the magnitudes and distribution of biaxial tensile and compressive stress components extending from the surfaces of torsion specimens to their neutral axes. A torsional stress diagram suitable for this purpose has been developed. It is similar to the conventional diagrams used to illustrate stress distribution through specimens loaded in bending and in direct tension or compression.

A plane intersecting a cylinder at an angle of 45 deg. is shown in Fig. 8. The width of the plane *OO'* is equal to and coincident with the diametral line *OO'* of the cylinder. The axis *XX'* of the cylinder and *WW'* of the plane intersect the diametral line *OO'* at *O"*. The angle *XO"W* is equal to 45 degrees.

When a twisting couple is applied to the cylinder, the tangential stresses through the specimen acting along either 45 deg. helix are assumed to increase in proportion to the radial distance from the *XX'* axis, where they are zero to maximums at the cylinder surface. Under a clockwise twisting couple, as indicated by the arrows on the cylinder, compressive stresses normal to the radial line *OO"* act in the direction of right hand helixes and lie in the plane *WPTW'*. *Tensile* stresses normal to the radial line *O"O'* act in the direction of left hand helixes and lie in the *WRLW'* plane.

In the diagram, compressive stresses will be shown to the right of the diametral line *OO'* in the plane *OTLO'*, and tensile stresses will be shown to the left in the plane *OPRO'*. With this diagram, the nominal tensile and compressive stress components from a twisting couple

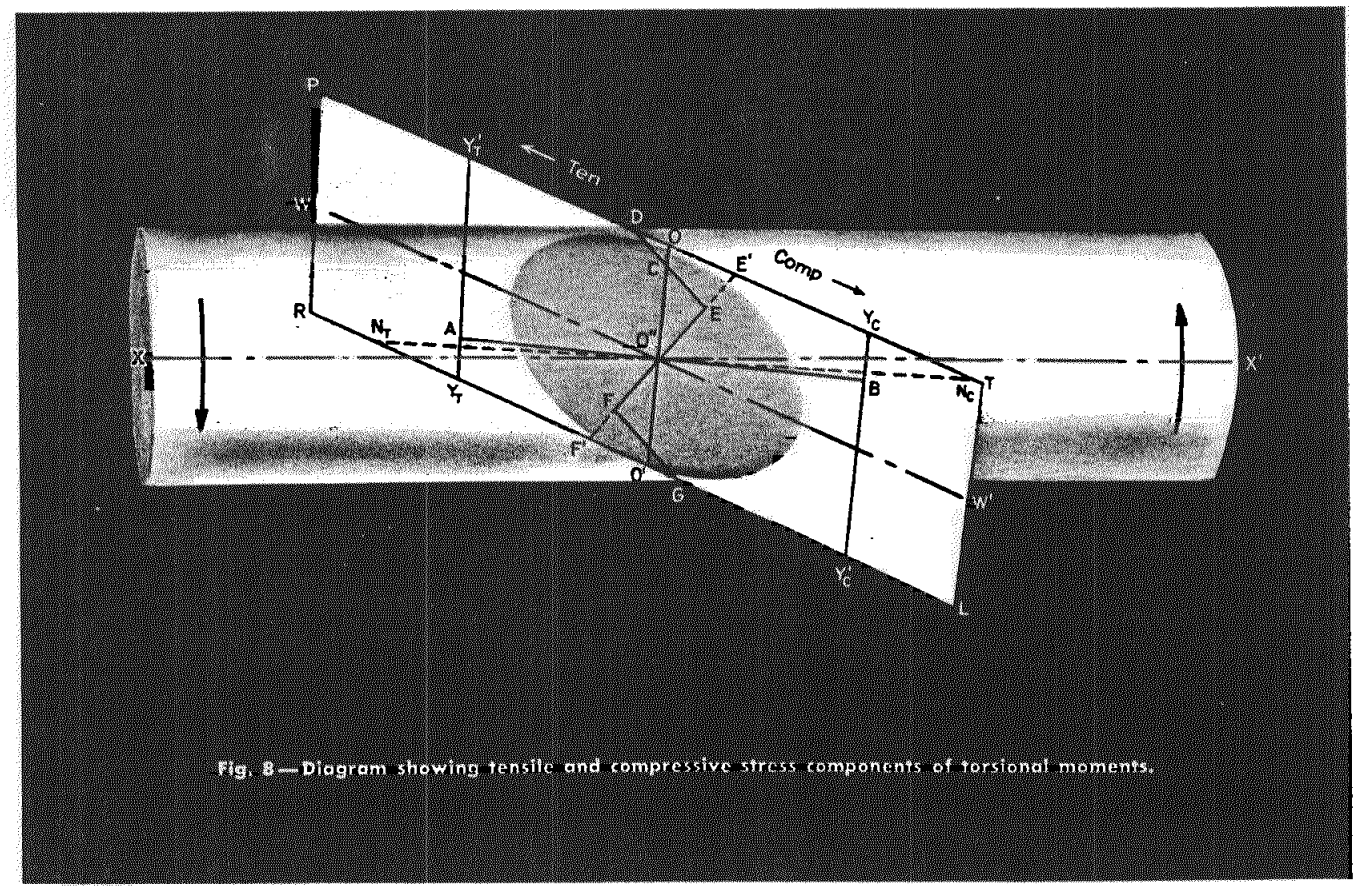

Fig. 8—Diagram showing tensile and compressive stress components of torsional moments.

may be expressed by the straight line N_iN_e in the plane $PTLR$ passing through the point O''. The stress at any depth within the cylinder is indicated by the perpendicular distance from the diametral line OO' to the nominal stress line shown on the diagram.

Stresses Are Biaxial

For straight cylindrical specimens loaded in pure torsion, the stresses at opposite ends of a diameter are correctly expressed in direction, sign and magnitude by the diagram because the stresses are symmetrically distributed with respect to the cylinder axis. In practice, however, few specimens are loaded in pure torsion, therefore, the stress patterns are variously distorted. The stresses at opposite ends of a diameter may not be identical and the neutral axes may not coincide with the specimen axis.

Since the diagram of Fig. 8 is designed to express biaxial stresses, it must always be remembered that the points O and O' actually represent a single point on the cylinder surface. The plane $WRLW'$ is in reality at a right angle to the plane $WPTW'$, as will be evident if the plane $WRLW'$ is rotated 180 deg. on the cylinder axis XX', at which time the radii OO'' and $O'O''$ will coincide. The arrangement shown in Fig. 8 is used as a means of simplifying the diagram.

Prestressing Induced by Torsional Overload

In the plane $PTLR$ of Fig. 8 is shown a diagonal line $N_iO''N_e$. This line represents the nominal tensile and compressive stress components acting normal to the diametral line OO' as a result of a clockwise torsional couple applied to the cylinder. The portion N_eO'', acting in the direction of a right hand helix, represents the range of compressive stress from zero at the point O'' on the cylinder axis to a maximum of ON_e at its surface. The portion N_iO'', acting in the direction of a left hand helix, represents the range of tensile stress from a value of zero at O'' on the cylinder axis to $O'N_i$ at its surface.

The compressive yield stress of the cylinder material is represented as the distance from the diametral line OO' to the parallel line Y_eY_e'. Likewise, the tensile yield stress is the distance from OO' to the tensile yield line Y_iY_i'. It is seen that the nominal stress N_eN_i from the applied torsional couple exceeds the surface compressive and tensile yield strengths by the quantities Y_eN_e and Y_iN_i respectively.

The triangular areas N_iY_iA and N_eY_eB represent material that was plastically deformed by yielding, the actual stress is therefore represented by the line Y_iABY_e. Note that to avoid unnecessary complications in this diagram any change in yield strength that may have resulted from the cold working during plastic yielding is neglected.

Upon release of the external twisting couple, elastic recovery returned the spring to its original state except for the permanent set that resulted from the residual stresses induced by plastic yielding. Elastic recovery necessarily proceeded until a state of equilibrium was attained between the clockwise and counter-clockwise twisting moments. This condition is indicated by the zig-zag line $DEFG$. Since the specimen, Fig. 8, is a straight round bar loaded in pure torsion, equilibrium is attained when the clockwise torsional moments represented by the area ODC and the counter-clockwise moments represented by the area CEO'' are equal.

Residual Stress From Plastic Yielding

If no permanent set has occurred, the line EF would coincide with line OO' when the external twisting couple was removed. The deviation of the line EF, therefore, may be used as a measure of the permanent set. Permanent set is equal to the angle imparted to the specimen by an external twisting couple that will biaxially stress a point on the cylinder surface with the compressive component OE' and the tensile component $O'F'$.

Stresses represented by OD and $O'G$ are the biaxial residual stresses that were developed at any point on the surface of the specimen as a result of plastic yielding. Compressive yielding equal to Y_eN_e resulted in tensile residual stress equal to OD. Tensile yielding equal to Y_iN_i resulted in compressive residual stress equal to $O'G$. Note that these residual stresses are opposite in sign to the respective stresses that were applied by the external twisting couple, and that they are greatest when the externally applied load is at its minimum.

Fatigue From Residual Tensile Stress

In many cases, the residual tensile stress OD becomes great enough to initiate fatigue cracks. Such cracks grow more slowly than cracks that are initiated by external loads because the stress decreases with depth until, at a depth somewhat less than is represented by OC, their inward progress is stopped by insufficient tensile stress or by encountering compressively stressed material.

While the torsional stress diagram is identical in form with stress diagrams representing beams loaded in bending, it must be remembered that the torsional diagram represents the two components of biaxial stresses normal to a common radius; whereas the bending stress diagram represents stresses in a beam on opposite sides of the neutral plane.

Although the torsional diagrams that follow will not include the cylinder shown in Fig. 8, the ellipse of intersection may be retained as a mark of identification to distinguish between bending stress diagrams and torsional stress diagrams.

Cause of Abnormal Fatigue Cracks

Returning now to the coil spring, Fig. 6, it will be recalled that, considering only the nominal stress in the spring, the numerous abnormal cracks as at D appear to have been caused by compressive stresses. But since compressive fatigue cracks are impossible, it became necessary to discover sources of tensile stresses acting in the direction of nominal compressive stresses of sufficient magnitude to produce the observed cracks.

During the discussion of the biaxial torsional stress diagram, Fig. 8, it was shown that, qualitatively, the required residual tensile stress OD was developed as a result of the plastic yielding that occurred upon the application of the overload N_eN_i. A similar diagram representing the residual stresses from overloading the spring, Fig. 6, would be expected to supply even more interesting information.

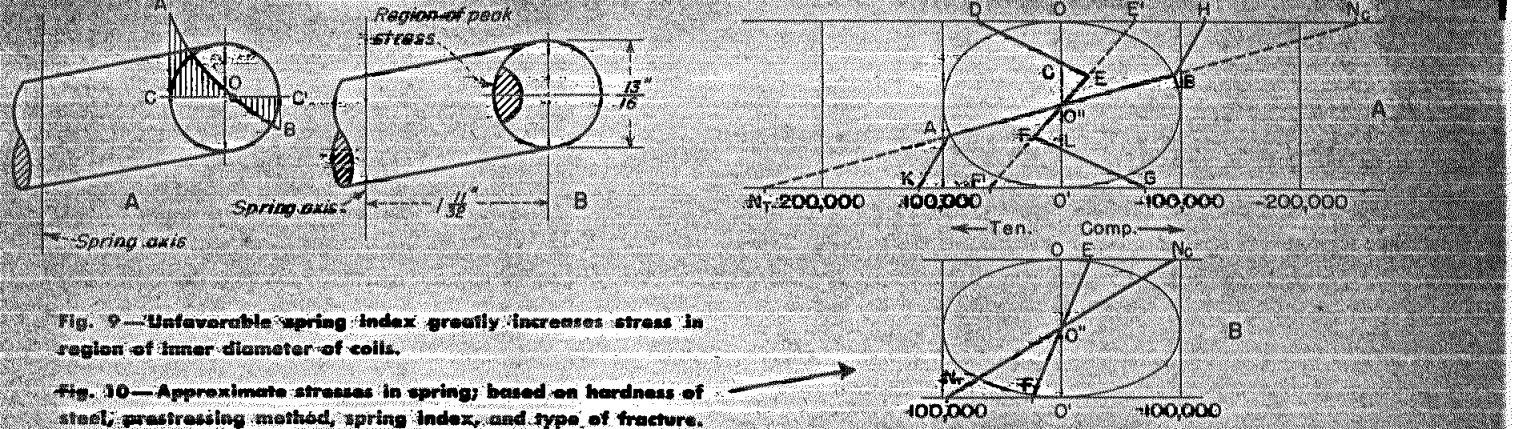

Fig. 9—Unfavorable spring index greatly increases stress in region of inner diameter of coils.

Fig. 10—Approximate stresses in spring; based on hardness of steel, prestressing method, spring index, and type of fracture.

Reconstruction of Residual Stresses

Although dissection stress analysis of this spring has not been made, and little is known regarding the magnitude of the processing overload stresses, or the stresses that resulted from service loads, it is nevertheless possible to reconstruct the residual stresses with sufficient accuracy to show the cause of the abnormal fatigue cracks.

From the hardness of the steel its yield stress may be estimated; from the dimensions of the spring and the measured depth of the fatigue crack at *D*, Fig. 6 (*B*) the depth of the residual tensile stress can be judged; and from the character of the mechanism in which it was used it can be appreciated that inertia extension loads were possible.

The pre-setting operation was stated by the manufacturer to have reduced the free height of the spring 3/16 in. To understand how so small a permanent set could result in large residual stresses, it will be necessary to consider the effects of spring dimensions on the magnitudes and distribution of stresses in this particular spring.

Effects of Low Spring Index on Stress Distribution

The diagrams Figs. 9 (*A*) and (*B*) have been prepared in accordance with the theories and test data of Wahl (Ref. 1) to show the distribution of stresses in the elastic range along a transverse diameter of the steel bar forming the spring, Fig. 6. In Fig. 9 (*A*), it is seen that the stress *CA* on the inner diameter of the coils exceeds the stress *C'B* on the outer diameter by more than 2.5 to 1. Note also that the point *O* of zero stress lies a considerable distance outside the center of the bar.

In diagram Fig. 9 (*B*) is shown that the peak stress is concentrated in a relatively small area near the inner circumferences of the coils. This unfavorable stress distribution results from the forming of proportionately small diameter coils from a bar of large diameter, that is, a spring having the very low index of 3.5.

Applying the torsional stresses shown in the conventional transverse shear stress diagram Fig. 9 (*A*) to biaxial torsional diagrams of the type described in Fig. 8, the diagrams Figs. 10 (*A*) and (*B*) are obtained. These diagrams show, in biaxial terms, the same stress relationships that are represented in Fig. 9 (*A*). Fig. 10 (*A*) presents the greater stress range of Fig. 9 (*A*) from the neutral axis at *O* to the inner diameter of the coil at *C*, and Fig. 10 (*B*) presents the lesser stresses in Fig. 9 (*A*) from the neutral axis at *O* to the outer surface *C'* of the coil.

The nominal biaxial pre-setting stress on the inner diameter of a coil is approximated in Fig. 10 (*A*) by the diagonal line N_tN_c, of which $O''N_c$ represents the compressive stress component ranging from zero at the neutral axis to a maximum of 250,000 psi at the surface, and $O''N_t$ represents the tensile stress component through the same range.

Yield Stress Estimated From Hardness of Specimen

Tests showed that, below a decarburized layer, the steel ranged in hardness from 45 to 47 Rockwell C, from which it was estimated that the initial tensile and compressive yield stress was 95,000 psi as is indicated at *A* and *B*. These yield stresses are assumed to increase to 120,000 psi at the surface along the lines *AK* and *BH* as a result of cold working during extensive plastic yielding. By these assumptions the broken line *KABH* represents the actual stresses from the pre-setting overload.

Upon release of the external load, elastic recovery returned the spring to its original height except for the 3/16 in. permanent set that resulted from plastic yielding. The magnitude and depth of plastic yielding is indicated by the triangular areas N_cHB and N_tKA which, respectively, represent compressive and tensile yielding. It will be understood that, because of the distorted stress pattern shown in Fig. 9 (*A*), the magnitude and depth of plastic yielding varied continuously around the circumference of the bar from a maximum, as shown in Fig. 10 (*A*), to no yielding at all for the diametrically opposite location represented in Fig. 10 (*B*).

In the straight cylindrical specimen represented by the diagram Fig. 8, equilibrium conditions were satisfied when the sum of the clockwise and counter-clockwise torsional moments represented in the single diagram were equal to zero.

It is not possible, however, to represent in any single diagram the residual stresses in a coil spring or other specimen in which the stresses are not symmetrically distributed. In such specimens, integration of positive and negative moments of a section is necessary to represent its precise equilibrium conditions. In view of the nature of the present problem, however, estimates of residual stress magnitudes from the two diagrams (*A*) and (*B*) of Fig. 10 will be sufficiently accurate for all practical purposes. This figure will be discussed further.

Equilibrium Condition Established

As previously stated, the diagram Fig. 10 (*B*) represents the biaxial stresses in the opposite side of the spring bar from the stresses shown in Fig. 10 (*A*). Since the latter stress is more than 2.5 times as great as the former, the applied stress N_tN_c of Fig. 10 (*B*) does not exceed the yield stress of the metal at any point.

Equilibrium in the free spring is assumed to be established when the clockwise torsional moments, represented by the residual stress areas *CEO"* and *LFO"* of Fig. 10 (*A*) plus the areas *OEO"* and *O'FO"* of Fig. 10 (*B*), are equal to the counterclockwise torsional moments, represented by the areas *OCD* and *O'GL* of Fig. 10 (*A*). By inspection these conditions are estimated to be satisfied by the residual stresses shown in the diagrams (*A*) and (*B*) of Fig. 10.

Mention has been made of a decarburized layer on the surface of the spring, the hardness of which was measured as low as Rockwell C 35. To indicate other effects than relative weakness of this soft layer, the diagram Fig. 11 (*A*) has been prepared. This diagram is the same as that of Fig. 10 (*A*) except that the yield stress of the surface is reduced to correspond to its measured hardness. It is seen that compressive and tensile yield strengths of the cold worked metal are reduced by an estimated 40,000 psi from *OH* and *O'K* to *OH'* and *O'K'*.

Decarburization Increased Residual Stress

Upon release of the external load, the added yielding appears as increased biaxial residual stresses *GG'* and *DD'*. These, like the previously described residual stresses in the metal near the inner diameter of the coils, are of opposite sign to the nominal biaxial stresses from the applied load.

With the added surface yielding, the residual stresses are represented in the diagram Fig. 11 (*A*) by the broken line *G'GFEDD'*. The yield stress of the carburized surface after cold working, however, was estimated to be 80,000 psi, which establishes this value as a limit of residual stress magnitude.

Much of the added surface residual stress shown in Fig. 11 (*A*) is therefore lost when the spring is unloaded, and the residual stress appears as the broken line *G'GFEDD'* in the diagram Fig.11 (*B*). This diagram is a representation of the probable stress range experienced by the spring, Fig. 6. In designing the spring the manufacturer calculated, by the Wahl formula (Ref. 1), that the load applied in service would stress the inner surface of the coils slightly less than 100,000 psi. The dashed diagonal line N_tN_c, Fig. 11 (*B*), therefore represents the calculated nominal service stress. The actual applied stress, which is represented by the broken line *K'KABHH'*, of course, is the algebraic sum of the nominal service stress and the residual stress.

Actual Stress Range Opposite to Nominal Stress Range

The stress range for both stress components is indicated by horizontal lines between the residual and the applied stresses of Fig. 11 (*B*). These show that the surface stress in the direction of the nominal compressive component ranged from 20,000 psi compression to 80,000 psi tension; and that the surface stress in the direction of the nominal tensile component ranged from 20,000 psi tension to 80,000 psi compression. This condition is seen to be almost a complete reversal from the nominal stresses in the extra vulnerable (Ref. 2) surface metal.

In addition to the stresses accounted for in the diagram, Fig. 11 (*B*), are possible biaxial stresses from rebound inertia when the applied load was suddenly released. The inclusion of such stresses up to 20,000 psi would not alter the magnitude of the surface stresses as represented in the diagram. They would only replace the remaining residual stresses from surface yielding *DD'* and *GG'*, which would be dissipated in the process.

From the foregoing it is seen that the numerous cracks on the inner surface of the coil spring, Fig. 6, which by superficial inspection appeared to have been caused by the compressive stress component of torsional loads, are in fact normal tensile fatigue failures. They demonstrate again that fatigue failures are tensile failures.

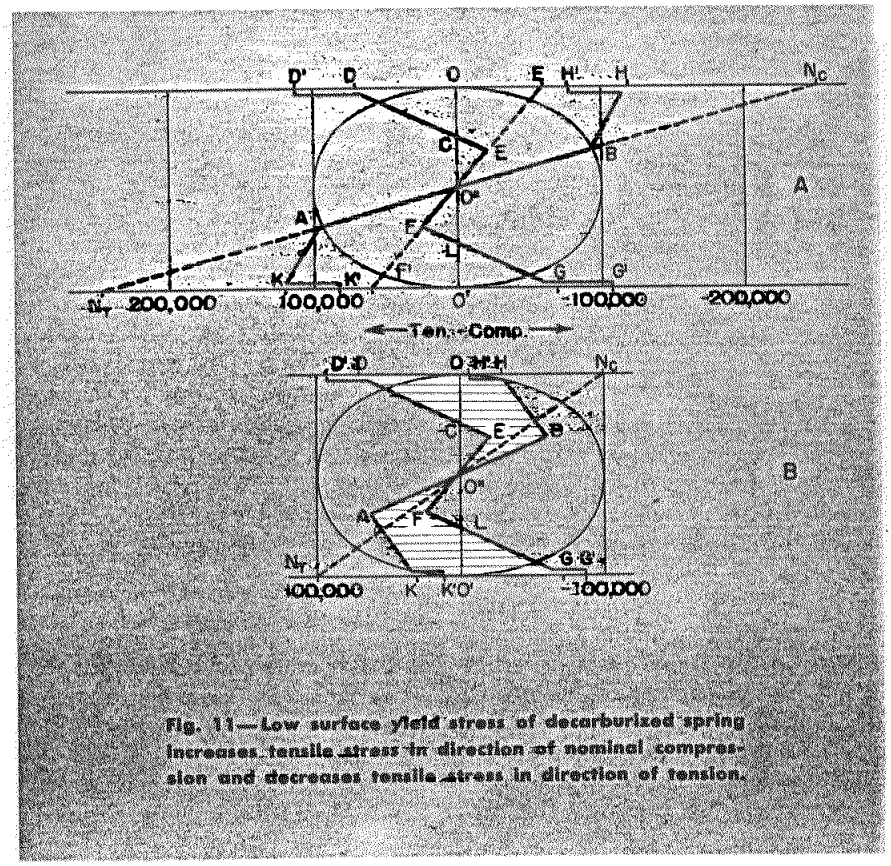

Fig. 11—Low surface yield stress of decarburized spring increases tensile stress in direction of nominal compression and decreases tensile stress in direction of tension.

Development of Fatigue Cracks

Having demonstrated that the numerous "compressive" fatigue cracks are actually tensile failures, it remains to show why so many non-fatal cracks formed in a single specimen, since it is usually found that a single crack grows to complete failure before another forms.

The numerous fatigue cracks developed because the depth of each crack was limitd by underlying compressively stressed metal. Referring to Fig. 11 (*B*), it is seen that the residual tensile stress that was responsible for the cracks is enclosed in the triangle *OD'C*. Each crack originated at the surface from the tensile stress *OD'*. As the depth of a crack increased, the tensile stress decreased until at *C* further progress is stopped because the stress, normal to the crack, became compressive (Ref. 3).

Since the tensile stress decreased with depth, the cracks advanced at a decreasing rate. Their progress presumably stopped shortly before reaching the point *C*, unless rebound inertia was great enough to momentarily increase the depth of the tensile stress and thus depress this point. Evidence of slow growth is seen in the smooth surfaces of such residual stress cracks, one of which is exposed at *D*, Fig. 6 (*B*).

The depth of the crack at *D* supplies a means of checking the accuracy of the assumptions made in constructing the diagrams Figs. 10 and 11, because the crack depth should correspond to the depth of the residual tensile stress *OC* in these diagrams.

The measured depth of the crack was 0.24 in., and the measured radius of the spring bar was 0.401 in. but, as shown in Fig. 9 (*A*), the distance from the surface at *O* to the neutral axis at *O''*, under stresses within the elastic range, is greater than the radius of the bar by approximately 0.06 in. The depth of the neutral axis *OO''* in Fig. 9 (*A*), therefore, may tentatively be taken as 0.46 inch.

The metal on the inner surface of the spring, however, experienced extensive plastic yielding during the pre-setting operation, as shown in Fig. 10 (*A*), the distance from the surface to the neutral axis was further increased to perhaps as much as 0.5 in. The depth of the residual stress *OC*, Fig. 11 (*B*), should be in nearly the same ratio to *OO''* of the same diagram as the measured crack depth is to the depth of the neutral axis, that is, *OC/OO''* is approximately equal to 0.24/0.5. With or without allowance for inertia stresses the agreement is seen to be very good.

Crack Growth Rapid

The behavior of fatigue cracks originating from the externally applied tensile stress is very different from the residual tensile stresses that have been discussed. Consider the tensile stress component of the external load in either diagram of Fig. 11. Assume a crack to be initiated by the tensile stress *O'K'*. As the crack depth increases, the tensile stress increases because the same external load must be supported by a decreasing area of metal. The rate of growth is therefore increased with crack depth and complete failure follows so quickly that rarely does a second crack have time to form.

Evidence of the increasing rate of growth of the fatigue fracture caused by externally applied tensile stress at *C*, Fig. 6 (*B*), is seen by the increasing roughness as this catastrophic crack advanced.

The presence of one or several cracks normal to the nominal compressive component did not greatly alter the functioning of the spring, Fig. 6, because the externally applied load acted to close the gaps and its behavior under load remained nearly normal. Continued operation initiated additional cracks that appeared at regularly spaced intervals, because as each crack formed the residual tensile stress was reduced for a distance on either side, and a new crack could not form in the stress relieved metal.

As each crack was formed the free height of the spring increased slightly because some of the residual stress that contributed to its permanent set was removed.

Moderate Versus Severe Pre-Setting

In Figs. 9 and 11, it has been seen that the numerous pseudo-compressive fatigue cracks in the spring, Fig. 6, were caused by residual tensile stresses that developed from excessive local plastic yielding during pre-setting. Although, under unidirectional loads such cracks seldom propagate to complete failure, it is nevertheless important to show the more desirable effects of moderate pre-setting in springs of high index. For this purpose, assume a spring similar in every respect to the spring diagrammed in Fig. 11 (*A*) except that the maximum nominal pre-setting stress is reduced from 250,000 psi of the former to 140,000 psi, as is shown by the diagonal line N_1N_2 of Fig. 12 (*A*).

Note that the actual applied surface compressive stress *OH'* and tensile stress *O'K'* are only slightly reduced from the corresponding stresses in Fig. 11 (*A*) but the permanent set, which is measured by *OE' and O'F'* in the respective diagrams, is greatly reduced. The lower permanent set has the effect of reducing the corresponding nominal residual stresses *OD'* and *O'G'* from the nominal value of 110,000 psi in the more severely processed spring to 54,000 psi in the moderately pre-set spring.

Under the same unidirectional operating loads that were applied to the severely pre-set spring, Fig. 11 (*B*), in which the maximum residual tensile stress *OD'* is seen to be reduced from 110,000 to 80,000 psi by local yielding, the equivalent stress in the milder pre-set spring Fig. 12 (*B*) is only 54,000 psi.

The corresponding surface tensile stress *O'K'* in the direction of the nominal tensile component of the applied load is seen to have increased from 20,000 psi in Fig. 11 (*B*) to 46,000 psi in Fig. 12 (*B*). It is, of course, possible to select a pre-setting load that will, under the nominal unidirectional test load of 100,000 psi, produce residual tensile stress equal to the actual applied tensile stress, in which case each would be 50,000 psi.

Since fatigue cracks originating from applied tensile stresses quickly grow to catastrophic proportions, whereas cracks from residual tensile stresses are relatively harmless, it is advantageous to reduce the former stress at the expense of the latter, as shown in Fig. 12 (*B*). In the diagrams Figs. 11 (*B*) and 12 (*B*),

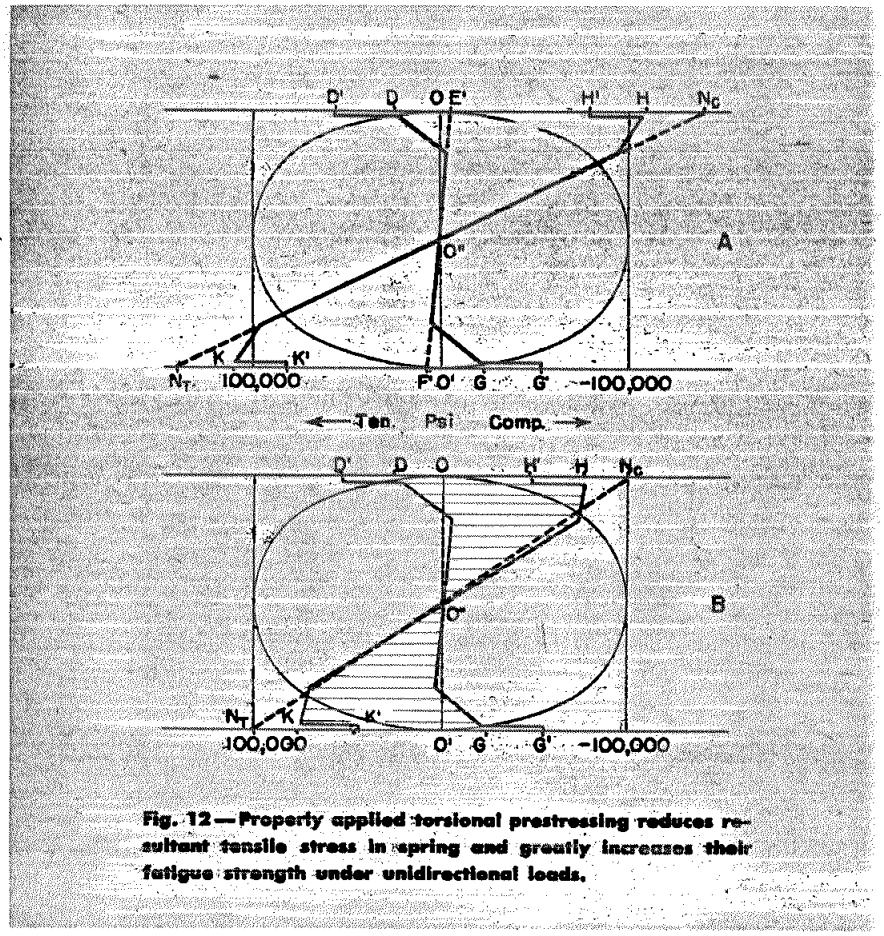

Fig. 12—Properly applied torsional prestressing reduces resultant tensile stress in spring and greatly increases their fatigue strength under unidirectional loads.

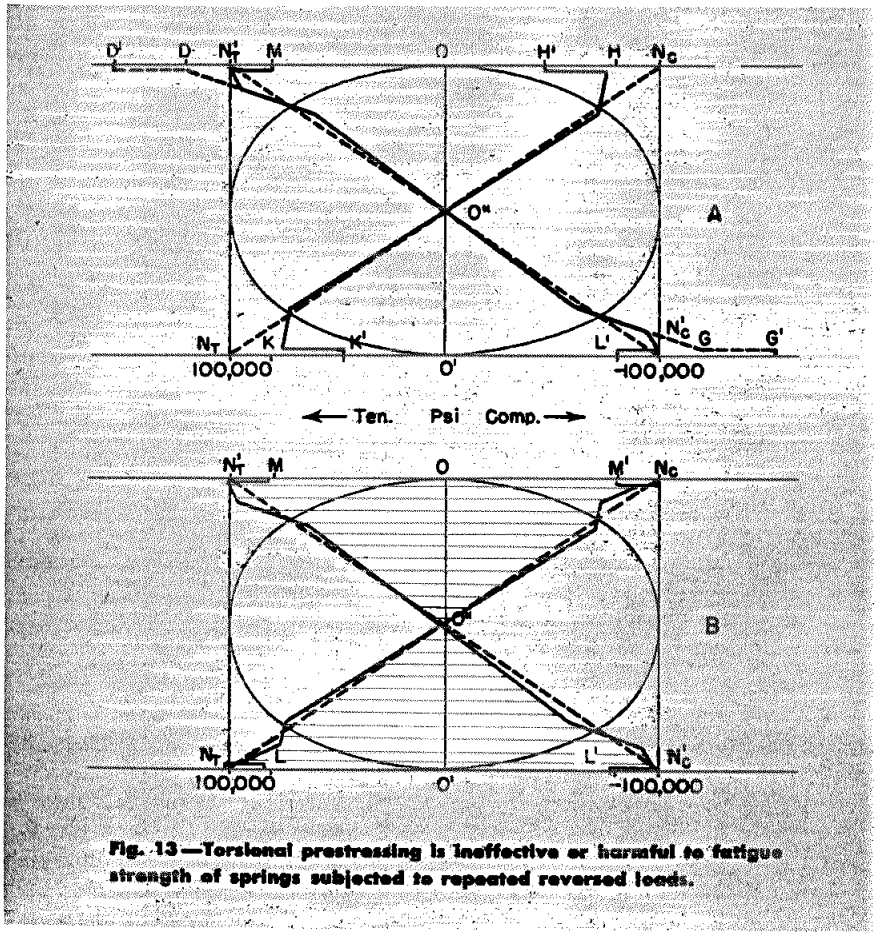

Fig. 13—Torsional prestressing is ineffective or harmful to fatigue strength of springs subjected to repeated reversed loads.

the operating stress ranges acting in the directions of both right and left hand helixes throughout the specimens are also compared.

Note in both Figs. 11 (*B*) and 12 (*B*), that the lower yield strength of the soft decarburized layers decreased the magnitudes of the dangerous tensile stress components from externally applied unidirectional loads by the amounts *KK'*. It is not known whether this stress reduction is sufficient to compensate for the lower fatigue strength of the decarburized steel, but the ill effects of decarburization are at least diminished.

Pre-Setting May Be Ineffective

Under reverse loading, whether the specimen is loaded in torsion or bending, this compensation cannot function because pre-setting in one direction will only increase the harmful stresses when the load is reversed. This qualification, as is shown in the diagrams Fig. 13, demonstrates again the fallacy of measuring fatigue strength by arbitrary test procedures and accounts for much confused thinking regarding fatigue of metals.

Assume a spring identical with the spring described in the discussion of Fig. 12 including the presetting operation; the only difference being that instead of unidirectional loading the applied loads will be repeatedly reversed.

After the prestressing operation the first load applies the nominal stress N_tN_t, which produces the actual stress $H'HKK'$ as shown in Fig. 13 (*A*). These stresses are seen to be identical with the corresponding stresses in Fig. 12 (*B*), since in both diagrams the loads applied to this point have been alike.

When the load is reversed, the nominal applied stress is that which is indicated by the dashed diagonal $N'_tN'_t$ of Fig. 13 (*A*). Except for plastic yielding, the change in actual stress will of course be equal to the change in nominal stress as is indicated by the broken line *D'DGG'*. But since this change exceeds the yield stress of the decarburized layer by the amounts *D'M* and *G'L'*, and of the harder underlying steel by the amounts DN'_t and GN'_t, plastic adjustment must occur by which the actual stress becomes MN'_t N'_tL'.

After a few reversals the operating stress range will be approximately that which is shown by the horizontal lines in Fig. 13 (*B*). This stress range is seen to approximate the range of the nominal applied stress, as indicated by the dashed line, except for repeated plastic yielding of the decarburized layer.

Yielding occurs with each load reversal because the applied surface stress ranges from plus 100,000 psi to minus 100,000 psi, but the yield strength of the decarburized layer is 80,000 psi in either direction. Plastic yielding of the decarburized layer must therefore occur with each load reversal as indicated by the stresses N'_tM, N_tM', N_tL, and N'_tL' of Fig. 13 (*B*) unless the applied nominal stress is reduced to 80,000 psi or less.

A comparison of the tensile stress magnitudes in Figs. 12 (*B*) and 13 (*B*) shows why fatigue strength is greater under unidirectional loads than under reversed loads as is empirically expressed by diagrams of the Goodman type. It will also show why some experimenters find prestressing treatments of little or no value, while others find such operations indispensable.

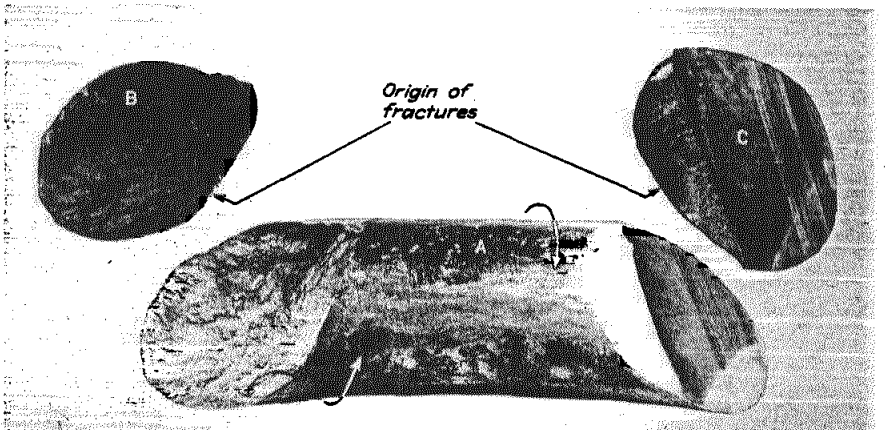

Fig. 14—Fatigue failures of coil springs. Note opposite diagonals of fractures from (B) tensile stress and from (C) "compressive" stress.

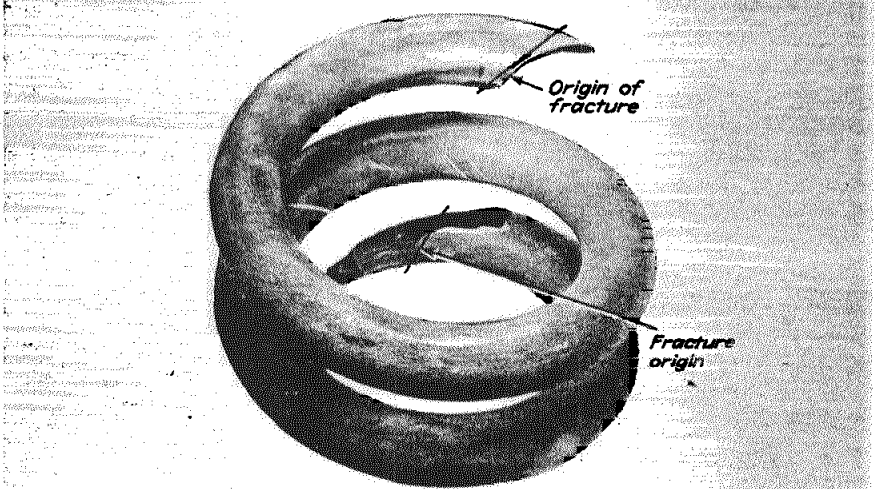

Fig. 15—Experimental locomotive suspension spring shows two left hand helix fatigue fractures from service loads and several right hand helix fatigue cracks from residual tensile stress.

Railway Spring Failures

Fatigue failures of coil springs having fractures normal to the nominal tensile stress component, and pseudo-compressive fatigue cracks extending in the direction of the opposite helix as shown in Fig. 6, frequently occur in railway equipment. Since the pseudo-compressive cracks rarely develop to complete fracture, they are seldom discovered because usually they can be detected only by magnetic or black light inspection of springs after considerable service use.

The short section of a coil spring shown in Fig. 14 was cut from a railway car suspension spring, which had been removed because of the catastrophic fatigue fracture originating on the inner surface of a coil, as is shown at the left of the portion *A*. Although there was no reason to suspect additional cracks, the spring, which was donated to the author's "scrap pile" by a railway repair yard, was subjected to magnetic particle inspection. This inspection quickly disclosed a short "compressive" crack, also on the inner surface of the coil, a short distance from the normal catastrophic fracture.

To disclose the dimensions of the crack, a grinding cut was made from the opposite side of the bar near the plane of the crack and the remaining section was broken, as shown at the right of the portion *A*. Photograph *C* of Fig. 14 was made normal to the plane of grinding to better show the characteristics of the pseudo-compressive crack. The well defined "fish scale" markings show that the crack advanced slowly from the inner surface of the coil to its final depth, which was found to be one-sixth the diameter of the bar.

Since this crack was caused by residual tensile stress, it may be concluded that its depth represents the approximate depth of the residual tensile stress, and that its further progress was stopped by underlying compressive stress, as is shown at *C* in the diagrams of Figs. 11 (*A*) and (*B*). No doubt this crack had reached its final depth long before the catastrophic crack commenced.

The photograph *B*, Fig. 14, shows details of the normal fracture that was caused by the tensile stress component of the externally applied load. The absence of well defined

"fish scale" markings shows that the initial crack propagated quickly to complete failure with relatively few load applications.

Residual Stress From Service Loads

Specification for material, heat-treatment and processing are not available but it is doubtful that this spring was intentionally pre-set. It was made from a bar 1.3 in. dia., hot wound in coils 5.55 in. outside diameter, or a mean coil diameter of 4.25 in. The spring index, that is, the mean coil diameter divided by the bar diameter, was 4.25/1.3 or 3.27. This ratio is even more severe than that of the spring shown in Fig. 6, the index of which was 3.4. Nominal stress distribution, therefore, was similar to that shown in the diagram Fig. 9 (*A*) by which it was found that the stress on the inner surface of the coils was 2.5 times as great as the stress on the outer surface.

Sub-surface hardness was found to be Rockwell C 44-45, and the hardness of a decarburized surface layer to range from Rockwell C 25 to 35. Residual tensile stresses of sufficient magnitude to initiate a fatigue crack, and of sufficient depth to correspond to the depth of the pseudo-compressive crack shown in Fig. 14 (*C*), could develop from a few applications of overload in normal service.

An experimental railway suspension spring is shown in Fig. 15, which has two left hand helix fatigue fractures normal to the tensile stress components of the applied service load, and several right hand helix pseudo-compressive fatigue cracks normal to the nominal compressive stress components. This spring was hot formed from a bar of 15/16 in. dia. into coils of 5⅝ in. outside diameter. Its index was 5. Sub-surface hardness was found to be Rockwell C 47-49, and the decarburized surface hardness to be Rockell 33-35. The depth of the non-fatal crack at the right was 0.16 in. This specimen presents no unusual characteristics. It is shown only as additional evidence that torsional fatigue failures are tensile failures. Another interesting vehicular spring type consisting of straight steel bars loaded in torsion is sometimes used in place of coil or leaf springs, and is discussed in the next

Torsion Bar Springs

In Fig. 16 is shown a torsion bar spring extensively used in World War II in the suspension system of a military vehicle.

This spring is shown as it appeared after having been laboratory fatigue tested to failure by unidirectional loads applied in a clockwise direction. The reader can readily confirm the direction of the applied loads by noting the direction of the fracture at its point of origin. Since the fracture was caused by the tensile component of the applied loads it is seen that, just as in the case of the paper covered cylinder shown in Fig. 2 (*A*), the loads must have been in a clockwise direction.

These torsion bars were provided with splined enlargements 2.75 in. at each end, whereby the vehicle load was transferred from the track wheels through the elastic bars to their respective anchorages on the opposite side of the vehicle. The diameters of the effective elastic portions of the bars were 2.27 in. and their effective lengths between enlargements were approximately 72.7 in. They were made of NE9262 steel, heat-treated to uniform hardness of Rockwell C 49-50 through their sections. Surface decarburization was too shallow to be detected by indentation hardness measurements.

Prestressing Increases Strength

For the purpose of further increasing the compactness of this suspension system the torsion bars were, as final operations, prestressed by shot peening and by overloading (pre-setting) in the direction of the normal service load.

In a previous report concerning the same torsion bars, H. O. Fuchs and R. L. Mattson (Ref. 4) state that these pre-setting operations had the effect of increasing the initial yield strength of the bars from 115,000 to well over 140,000 psi with a correspondinng increase in their fatigue strengths. They also stated that: "The practical importance of raising the safe load stress from about 105,000 to 140,000 psi may be readily appreciated. Since space and weight requirements are inversely proportional to the square of the safe load stress, it amounts to saving almost half the space and weight which should be necessary without pre-setting."

The sequence in which the prestressing operations were applied was important, as is shown by the bar chart Fig. 17, which is re-plotted from a report issued by the National Defense Committee of the O.S.R.D. (Ref. 5). It is seen that the fatigue strength was much greater in torsion bars that were shot peened before pre-setting than when the opposite sequence was followed or when shot peening was omitted. Shot peening before pre-setting was more effective, presumably because it reduced the damage to the surface metal that would result from extensive tensile plastic yielding.

The pre-setting operations were performed by applying, through the splined ends, five successive torsional loads sufficient to twist the finished bars to the same end position of approximately ninety degrees from the original free position. In terms of nominal stress this twist was approximately 255,000 psi, which greatly exceeded the yield strength of the bars. As a consequence of extensive plastic yielding each bar developed a large permanent set.

Damage by Tensile Yielding

Since the hardness of the bars was Rockwell C 49-50 and their ductility correspondingly low, it is believed that the capacity of the unpeened vulnerable surface metal for tensile plastic adjusment was therefore reduced.

When shot peening preceded the pre-setting operation, the vulnerable surface became biaxially stressed in compression by an amount approximating one half of the yield strength of the steel. As a result of this residual compressive stress, no tensile plastic yielding occurred in the vulnerable surface and much or all fatigue damage was thereby avoided.

Shot peening did not alter the extent of tensile plastic yielding a short distance below the surfaces of the bars, but since sub-surface metal is apparently less vulnerable to damage by tensile plastic yielding than surface metal the loss of fatigue strength, if any, was small.

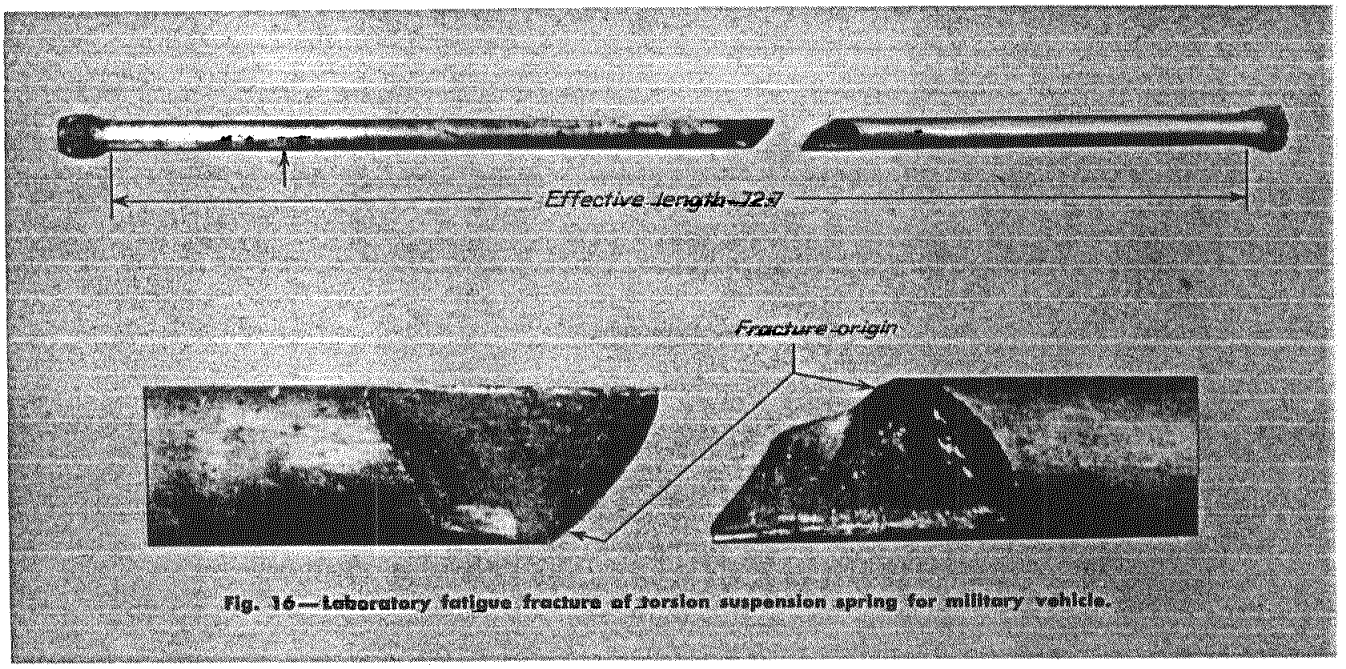

Fig. 16—Laboratory fatigue fracture of torsion suspension spring for military vehicle.

Because shot peening induced biaxial compressive stress in the affected layer, the compressive strain in the direction of the compressive component of the pre-setting load was increased. Plastic yielding in this direction was, therefore, more than doubled by the peening. But, as is shown in Fig. 17, if any damage resulted, it was less than the damage from the tensile plastic yielding in the unpeened bars.

Shot peening applied only after pre-setting was not effective because the damage from tensile plastic yielding had already occurred.

The measurement of effective residual stresses in torsion bars by the dissection method (Ref. 4) is discussed on the following pages. In only one were the measurements sufficiently refined to show the stress induced by shot peening and other important facts.

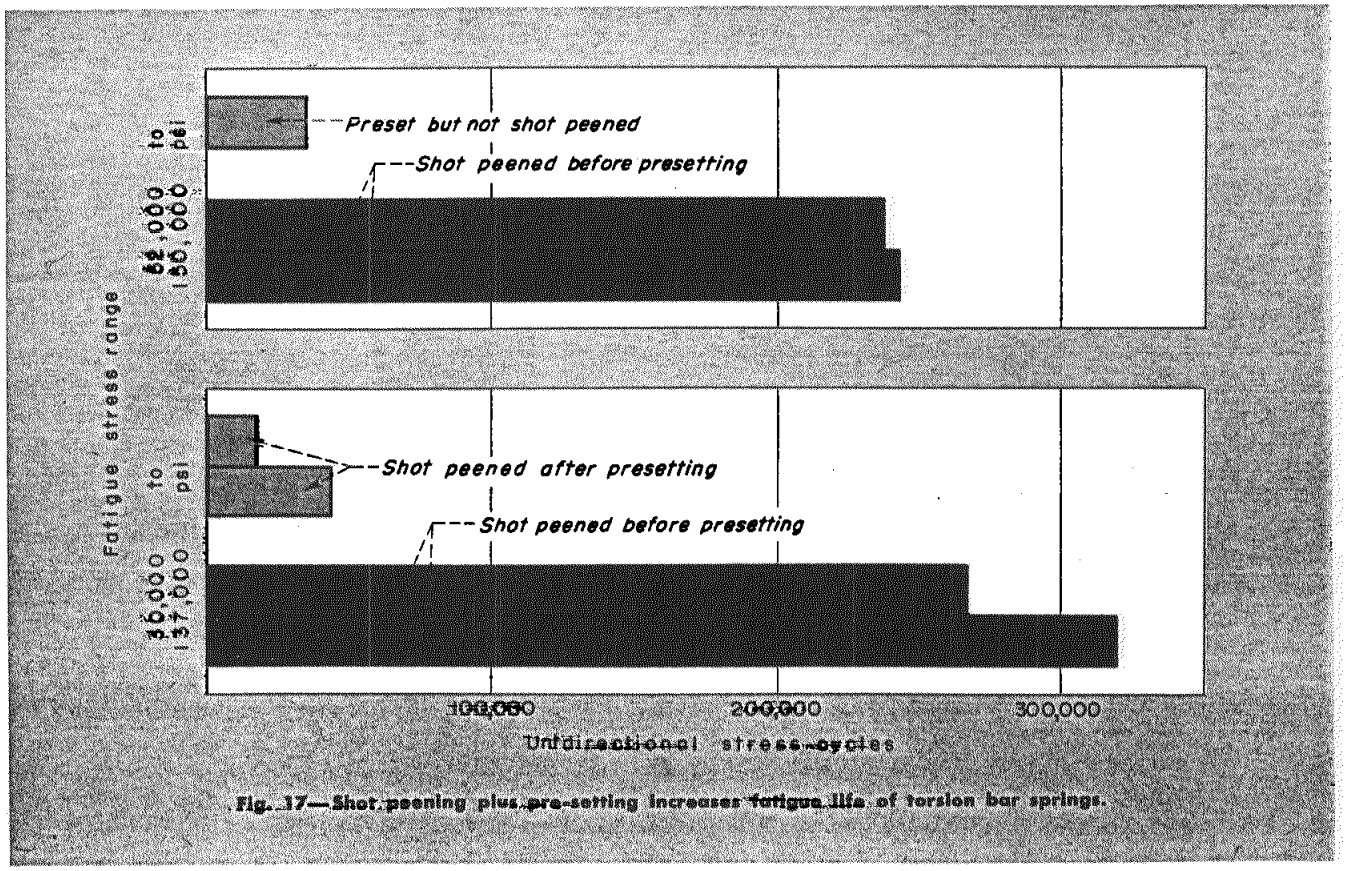

Fig. 17—Shot peening plus pre-setting increases fatigue life of torsion bar springs.

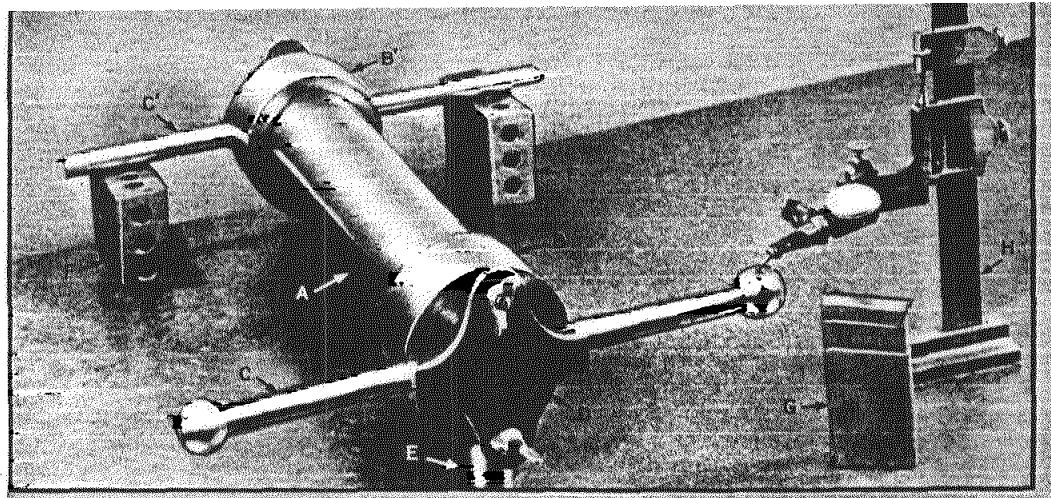

Fig. 19 — Setup for measuring angular changes in section of pre-set torsion spring after removal of successive surface layers.

Fig. 18 — Stress measurement by dissection — (A) 10 in. section cut from torsion bar. — (B) Same with V-caps after a few layers have been removed. — (C) Remainder after removal of all residually stressed metal.

Residual Stress in Bar Is Measured

To find the stress in a torsion bar measurements were made by grinding away successive layers of metal from the cylindrical surface of the bar, and measuring the resulting angle of rotation of one end of the specimen in relation to its opposite end. The magnitude of the residual torsional stress in each layer was equal to the torque necessary to hold the remainder of the bar in the angular relationship existing before the layer was removed.

As measured the specimen would not respond to the biaxial stress originally induced by shot peening, because this stress had no torsional component being compressive in both directions. The torsional overload that was applied after shot peening, however, caused unequal plastic yielding in the shot peened layer, which distorted the surface residual stress pattern so as to produce an additional torsional stress.

The specimen used for the dissection measurements is shown in Fig. 18. A ten inch section was cut from a full length torsion bar, Fig. 18 (*A*), and accurate centers were drilled in both ends. Ferrules containing V-grooves were pressed on both ends as shown at (*B*). The specimen was then ground away in 80 layers, which reduced its diameter from 2.27 to 0.662 in. as shown at (*C*). At this diameter all of the stressed metal had been removed.

The setup for measuring angular changes after the removal of each layer is shown in Fig. 19. Sine bars *C* and rest bar *C'* were clamped in the V-grooves of their respective ferrules. The rest bar *C'* and its end of the specimen were supported on the blocks *F-F'*, which were always located on marked areas on a surface plate. The near end of the specimen was supported at an equal height from the surface plate by the block *E*, which also occupied a marked spot on the surface plate.

The sine bar *C* was provided with spherical ends each spaced five inches from the center of the specimen. Both bars were located in their respective V-grooves by off center dowels to prevent any possibility of altering the location of either bar relative to the specimen.

Angular changes in the specimen were measured by determining the difference in height from the surface plate of the spherical ends of the sine bar *C*. The measurements were made by stacking Johansson gage blocks, shown at *G*, to the same height as the sphere being measured. The height of the gage blocks and the sphere were compared with a dial indicator attached to a surface gage.

To provide direct readings, the sine bar spheres were spaced ten inches apart so the differences in their heights were ten times the sine of the angle of rotation.

The surface of the torsion bar specimen between the ferrules was ground away in successive layers at a slow rate to avoid development of large magnitude residual tensile stresses. This precaution was observed although it was realized that uniform biaxial residual stresses of one sign would not contribute directly to the unwinding characteristics of the specimen. It was possible, however, that the heat of grinding would slightly alter the residual stress induced during processing in the remainder of the specimen after a layer had been removed and thus affect the residual stress measurements.

The length of the ground portion of the specimen ranged from 8.95 in. at the outer diameter, as shown in Fig. 18 (*B*), to 8.89 in. when the last layer was removed as shown in Fig. 18 (*C*).

Dimensional data relating to the

dissection processes are given in Table I. These data are given in considerable detail to indicate the painstaking accuracy that is considered essential in such studies.

It is seen that the thickness of the layers removed between measurements varies from approximately 0.001 in. near the original surface to 0.015 in. at greater depths. Special attention to the residual stress near the surface is necessary because of the greater vulnerability to fatigue and brittle failure of this portion of the specimen. Also, more frequent readings are required in regions in which rapid changes in residual stress are anticipated. When residual stress changes are small or of uniform magnitude the thickness of the layers may be increased. Unless the residual stress pattern is known with reasonable accuracy, however, important data may be lost by proceeding too rapidly.

The last column of Table I shows the angle of twist in seconds of arc for each layer of metal that was removed. This column is presented to demonstrate that in spite of the precautions taken in grinding and in measuring, the resulting angles of twist vary erratically. To overcome such variations, practice at the Research Laboraties Division of the General Motors Corporation is to make large scale plots of thickness of metal layer removed versus total deformation. A faired curve is then drawn to approximate the average of the test points, and corrected values of deformation for each layer are then taken from the faired curve.

The angle of twist in the remaining cylinder of the specimen is a measure of the mean stress in each layer removed because, prior to removal, each layer forcibly restrained the underlying cylinder from rotation through that angle. The mean stress in each layer removed is therefore that which would result from applying to the layer the torque necessary to twist the remaining cylinder through the measured angle. After the 81st layer was removed, the remaining metal was free of macro residual stress, as is indicated by the decreasing sine bar readings. The faired curve, referred to in the preceding paragaph, indicates that the diameter of zero residual stress was 0.630 in. and not 0.662 in. as is shown in Table I, first column.

Torsional residual stresses from the surface to the center of the specimen, calculated from the data in Table I, are shown by the curve *G'FO"* in Fig. 20, which is a conventional torsional stress diagram in which no distinction is made between tensile and compressive stresses.

The curve *G'FO"* is seen to cross the zero stress line *O'O"* at *C*, thus establishing the area *CFO"C* representing a clockwise torsional moment and the area *CG'O'C* representing a counterclockwise torsional moment. Since to satisfy equilibrium conditions, it is necessary that the sum of these torsional moments equal zero, the accuracy of the dissection measurements may readily be tested from known stresses and the radii at which they occur. It was found that

$$\frac{\text{Clockwise moment}}{\text{Counterclockwise moment}} = \frac{-SR^2\Delta R}{SR^2\Delta R} = 0.991$$

indicating an overall error of less than one percent. This statement does not mean that the errors in residual stress magnitude are less than one percent. It is extremely

Table I — Dissection Process Dimensional Data

Layer No.	Bar Dia, in.	Layer Thickness Removed, in.	Angle of Twist Per Layer, Seconds	Total Sine Bar Reading, in.	Layer No.	Bar Dia, in.	Layer Thickness Removed, in.	Angle of Twist Per Layer, Seconds	Total Sine Bar Reading, in.
0	2.270	0	0	0	41	1.8630	0.01525	176	0.111
1	2.267	0.0015	21	0.001	42	1.8340	0.0145	196	0.1205
2	2.2648	0.0011	0	0.001	43	1.8035	0.01525	185	0.1295
3	2.2626	0.0011	20	0.002	44	1.7735	0.015	186	0.1385
4	2.2600	0.0013	21	0.003	45	1.7430	0.01525	216	0.149
5	2.2575	0.00125	10	0.0035	46	1.7135	0.01475	165	0.157
6	2.2550	0.00125	31	0.005	47	1.6830	0.01525	227	0.168
7	2.2525	0.00125	10	0.0055	48	1.6535	0.01475	196	0.1775
8	2.2500	0.00125	11	0.006	49	1.6235	0.015	227	0.1885
9	2.2475	0.00125	10	0.065	50	1.5925	0.0155	217	0.199
10	2.2450	0.00125	31	0.008	51	1.5635	0.0145	217	0.2095
11	2.2425	0.00125	10	0.0085	52	1.5335	0.015	227	0.2205
12	2.2395	0.0015	11	0.009	53	1.5035	0.015	237	0.232
13	2.2370	0.00125	31	0.0105	54	1.4735	0.015	237	0.245
14	2.2350	0.001	10	0.011	55	1.4430	0.01525	279	0.257
15	2.2320	0.0015	10	0.0115	56	1.4120	0.0155	247	0.269
16	2.2285	0.00175	21	0.0125	57	1.3820	0.015	237	0.2805
17	2.2235	0.0025	31	0.014	58	1.3520	0.015	248	0.2925
18	2.2184	0.00255	10	0.0145	59	1.3220	0.015	167	0.306
19	2.2135	0.00245	31	0.016	60	1.2920	0.015	370	0.3185
20	2.2085	0.0025	31	0.017	61	1.2620	0.015	247	0.3305
21	2.2035	0.0025	21	0.0185	62	1.2320	0.015	248	0.3425
22	2.1937	0.0049	61	0.0215	63	1.2015	0.01525	299	0.357
23	2.1835	0.0051	62	0.0245	64	1.1720	0.01475	279	0.3705
24	2.1737	0.0049	31	0.026	65	1.1415	0.01525	268	0.3835
25	2.1633	0.0052	52	0.0285	66	1.1120	0.01475	248	0.3955
26	2.1534	0.00495	62	0.0315	67	1.0820	0.015	111	0.409
27	2.1385	0.00745	62	0.0345	68	1.0520	0.015	416	0.421
28	2.1235	0.0075	82	0.0385	69	1.0220	0.015	257	0.4335
29	2.0185	0.0075	62	0.0415	70	0.992	0.015	227	0.4445
30	2.0933	0.0076	93	0.046	71	0.961	0.0155	197	0.454
31	2.0786	0.00735	82	0.05	72	0.932	0.0145	196	0.4635
32	2.0635	0.00755	73	0.0535	73	0.902	0.015	144	0.4705
33	2.0435	0.0100	103	0.0585	74	0.8715	0.01525	166	0.4785
34	2.0235	0.0100	123	0.0645	75	0.842	0.01475	82	0.4825
35	2.0035	0.0100	114	0.070	76	0.812	0.015	83	0.4865
36	1.9833	0.0101	113	0.0755	77	0.782	0.015	62	0.4895
37	1.963	0.01025	124	0.0815	78	0.752	0.015	41	0.4915
38	1.9435	0.00975	114	0.087	79	0.722	0.015	41	0.4935
39	1.9235	0.0100	123	0.093	80	0.692	0.015	11	0.494
40	1.8935	0.015	196	0.1025	81	0.662	0.015	20	0.495

difficult to measure stress near the surface of a specimen and the stress magnitude in this region is subject to relatively large errors. Also, the dissection method can, at best, measure only macro stresses giving no indication of the sign or the magnitude of micro stresses that may be present.

Residual Stress from Plastic Yielding

Torsional residual stresses, represented by the line FG, were developed during processing as a result of plastic yielding when the torsion bar was subjected to the presetting overload. At the surface this stress $O'G$ is compressive and equal to 18,000 psi. The residual stresses represented by the line $O''F$ occurred in metal that had experienced no plastic deformation but was elastically stressed by the permanent set of the spring. The portion GG' of the residual stress equal to 14,000 psi is a remnant of the compressive stress induced during the shot peening operation, which was applied prior to pre-setting.

The point F on the residual stress line $O''G'$, Fig. 20, lies at a radius of 0.315 in., which as was shown by the faired curve is the limit of plastic yielding. This point marks the limit of elastic behavior of the torsion bar steel when the five presetting overloads, having maximum nominal surface stress values of 255,000 psi, were applied. The indicated yield stress

$$S_y = \frac{R\ \text{max}}{R\ \text{min}} \times S\,\text{max} = \frac{0.315}{1.135} \times 255{,}000 = 71{,}000\ \text{psi}$$

is a very low value for this steel, which had a hardness of Rockwell C 49. The question arises whether the initial torsional yield strength at this depth may not have been depressed through the action of radial and tangential compressive stresses.

Permanent Set Measurements

The angle of permanent set can be found from Fig. 20 by extending the line $O''F$ to intersect the surface of the specimen at F'. The stress scale shows this intersection to occur at 73,000 psi. The nominal angle of twist during pre-setting was given as 90 deg. (Ref. 4), but this value was arbitrarily reduced to 86 deg. by the author, equal to 255,000 psi nominal stress to allow for elastic and plastic losses in the splines and loading gear during overloading.

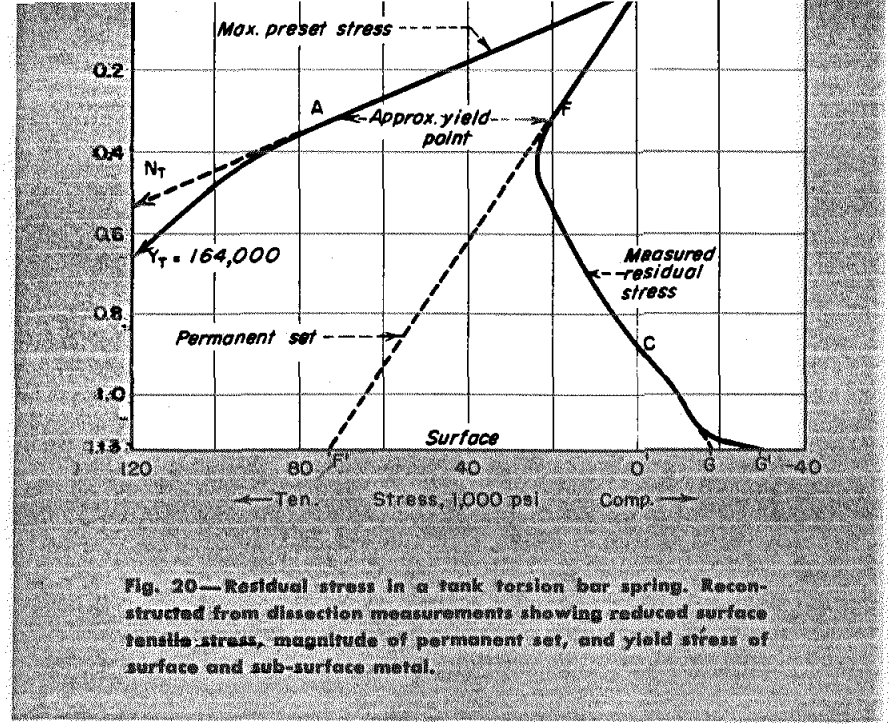

Fig. 20—Residual stress in a tank torsion bar spring. Reconstructed from dissection measurements showing reduced surface tensile stress, magnitude of permanent set, and yield stress of surface and sub-surface metal.

From these values the indicated permanent set angle is

$$\theta = \frac{73{,}000}{255{,}000} \times 86 = 24.5\ \text{deg}$$

The angle of permanent set may also be calculated from the final sine bar reading in column four of Table I and the ratio of effective length of the torsion bar to the length of the ground dissection specimen, Fig. 18 (C)

$$\sin\theta = \frac{72.7}{8.89} \times \frac{0.495}{10} = 0.4$$

$\theta = 23.5$ deg

This value is presumably more accurate than the preceding because it is obtained from the original test data.

Neither of these angular values agrees with the nominal permanent set angle of approximately 32 deg measured during processing (Ref. 4). There are reasons to suspect errors in the latter measurement but the angular magnitude of these probable errors cannot be accurately estimated.

It is also possible that changes occurred in the magnitude of the residual stresses during fatigue testing of the torsion bar spring prior to the dissection stress analysis. The bar from which the dissection specimen was taken was subjected to 70,000 stress cycles of unidirectional torsional loads at nominal stresses ranging from 20,000 to 145,000 psi. Although the torsion bar spring was not broken, a portion of the test fixture failed during the test. It is possible that a large negative torsional load was applied by the inertia of the bar and the attached splined loading members upon sudden release of the load.

Errors in permanent set angles, whatever their sources, would not alter the indicated initial yield strength of 71,000 psi but could have altered the magnitude of the surface yield stress obtained from the dissection stress data.

References

1. A. M. Wahl—"Mechanical Springs", Penton Publishing Company
2. J. O. Almen—"Fatigue Weakness of Surfaces", PRODUCT ENGINEERING, November 1950, p. 117.
3. J. O. Almen—"Fatigue Failures are Tensile Failures", PRODUCT ENGINEERING 1951, p. 101.
4. H. O. Fuchs and R. L. Mattson—"Measurement of Residual Stresses in Torsion Bar Springs", Society for Experimental Stress Analysis *Proceedings;* Vol. 4, No. I; 1946; p. 64.
5. R. K. Mattson and J. O. Almen—"Effect of Shot Blasting on Physical Properties of Steel," Final Report, Part II, O.S.R.D., No. 4825. Published by National Defense Committee of the Office of Scientific Research and Development, War Metallurgy Division, 1945, p. 23.

PART II

TORSIONAL FATIGUE FAILURES

J. O. ALMEN
Research Laboratories Division, General Motors Corporation

REPRINTED FROM MARCH 1952

PRODUCT ENGINEERING

A McGraw-Hill Publication
330 West 42nd St.,
New York 36, N. Y.

PART II

TORSIONAL FATIGUE FAILURES

J. O. ALMEN
Research Laboratories Division, General Motors Corporation

Analytical studies of fatigue fractures in torsion bar springs for military vehicles that, in spite of inherent planes of weakness, show that torsional fatigue failures are caused by and develop normal to the tensile component of the applied stress. Data bearing on the characteristics of torsional failures obtained from fatigue tests of torsion bars that were subjected to experimental variations in processing.

SUBSTANTIAL EVIDENCE was presented in the article "Torsional Fatigue Failures," PRODUCT ENGINEERING, September 1951, p 167, to show that tensile stress is the direct cause of fatigue failures from repeatedly applied torsional loads. Data presented in that article also show that the compressive stresses contribute to fatigue failure only in an indirect manner through altering the yield strength of the metal.

In the discussion on Torsion Bar Springs in the latter part of that article, data obtained by the dissection process were presented to evaluate the residual stresses in a specimen cut from a torsion bar spring, which was made of NE 9262 steel, heat-treated to a uniform hardness of Rockwell C49-50. In the final processing, these bars were prestressed by shot peening and by overloading in the direction of the normal service load.

It was seen that the fatigue strength was much greater in torsion bars that were shot peened before pre-setting than when the opposite sequence was followed or than when shot peening was omitted. In terms of nominal

Fig. 1—Residual stress in a tank torsion bar spring. Reconstructed from dissection measurements showing reduced surface tensile stress, magnitude of permanent set, and yield stress of surface and sub-surface metal.

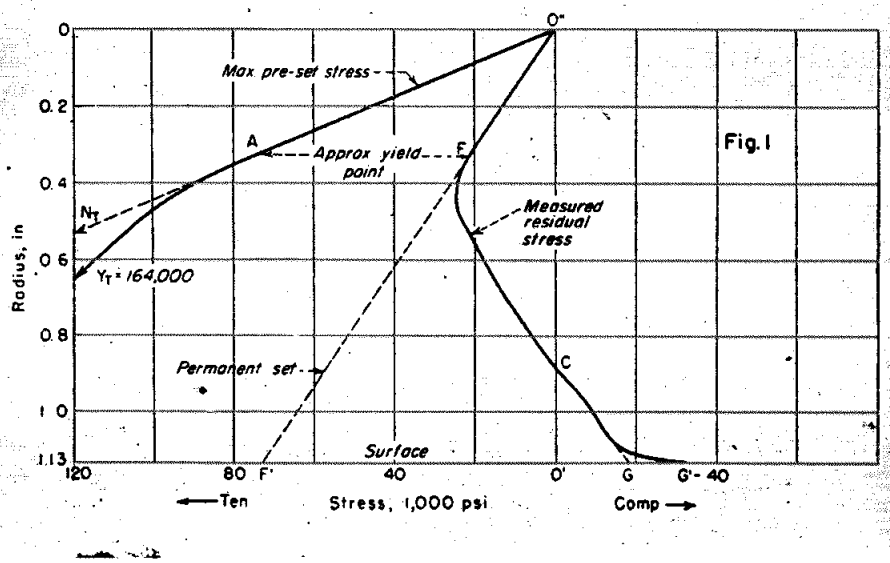

Fig. 2—Tank torsion bar spring diagrams. (A) Favorable residual stresses induced. (B) Loss during processing. (C) Resulting operating stress ranges.

stress, the twisting or pre-setting was approximately 255,000 psi, which stress exceeded the yield strength of the bars.

When shot peening preceded the pre-setting operation, the vulnerable surface became biaxially stressed in compression by an amount approximating one half of the yield strength of the steel.

The data as revealed by the dissection measurements on the torsion bar spring specimen are shown in Fig. 1. These data, together with an interpretation of them to a lower order of accuracy, are reported in Fig. 2. The diagrams of Fig. 2 also differ from Fig. 1 in that they present the data in terms of tensile and compressive stress components in the manner shown in Fig. 3. The construction of diagrams such as Fig. 3 were discussed in the September 1951 article. These diagrams show separately the magnitudes and distribution of biaxial tensile and compressive stress components extending from the surfaces of torsion specimens to their neutral axes.

The diagonal line N_tN_c Fig. 2(A) represents the nominal tensile stress compressive stress component N_tO'' and the compressive stress component $O''N_c$ that resulted from the torsional prestress of 255,000 psi. Each component is arbitrarily given the same value as the resultant torsional stress in Fig. 1. The point A on the diagonal N_tN_c indicates the initial sub-surface yield stress in the direction of the tensile stress component, and the point B indicates the initial sub-surface yield stress in the direction of the compressive stress component. Since diagram Fig. 2(A) expresses biaxial stresses, the points A and B are actually coincident (the stresses at these points correspond to the torsional yield stress at A in Fig. 1), and are presumably equal in magnitude.

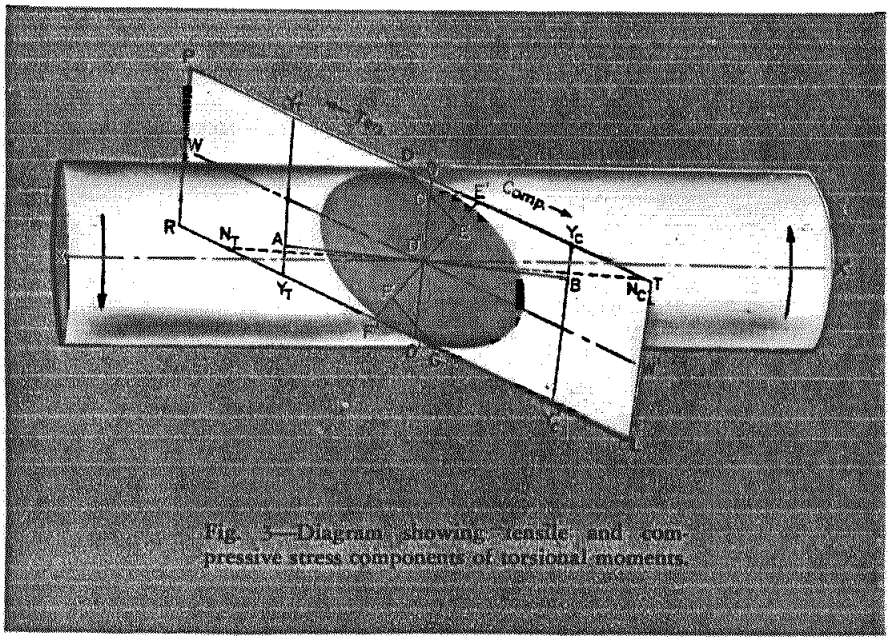

Fig. 3—Diagram showing tensile and compressive stress components of torsional moments.

Since the nominal torsional prestress N_tN_c exceeded the yield strength of the steel, the maximum surface stress was considerably less than 255,000 psi. Based on the residual stress data shown in Fig. 1, but not including the stress remnant GG' from shot peening, the surface tensile and compressive yield stresses were less than the nominal applied stress by an amount equal to the total plastic yielding $F'G$. By measurement, $F'O'$ equals 73,000 psi and $O'G$ equals 18,000 psi. From these data the extent of yielding in the direction of both components is taken as 91,000 psi. The surface yield strengths $O'Y_t$ and OY_c, Fig. 2(A), are therefore

$$255{,}000 - 91{,}000 = 164{,}000 \text{ psi}$$

The yield stresses at intermediate depths range from 164,000 psi at the surface to 71,000 psi at the depth A, somewhat as represented by the straight lines Y_tA and Y_cB.

The indicated yield strength of the cold worked surface metal, as well as the initial yield strength of sub-surface metal, is seen to be at variance with the values that would be expected from conventional yield stress determinations. This instance is the only one known to the author in which the pattern of torsional yield stress has been determined from residual stress measurements. The method appears to be inherently more accurate than the conventional method in which an assumed yield pattern is constructed upon static yield measurements. Additional dissection measurements of residual torsional stresses will be required to establish the relative merits of the two methods. This comparison should also be made for specimens that have been loaded above their yield strengths in bending, tension, and compression.

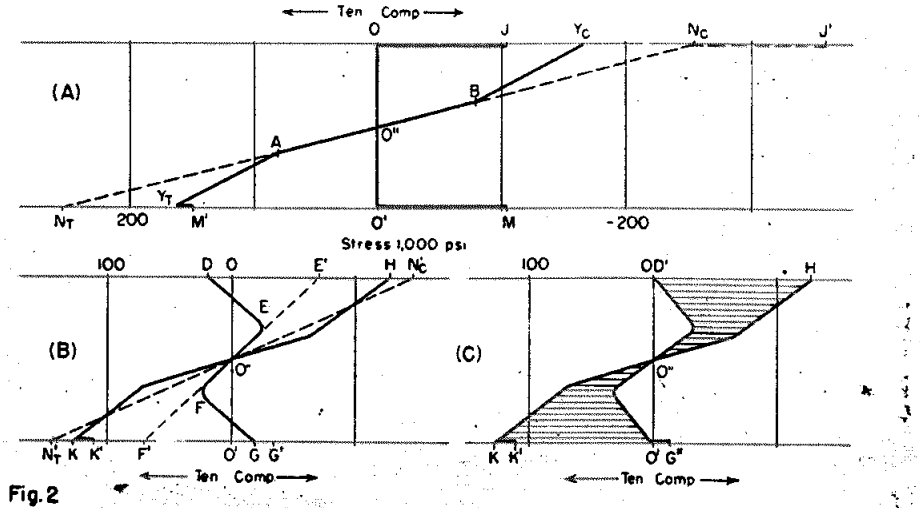

Fig. 2

Shot Peening Residual Stresses

Approximations of the biaxial residual stresses that were induced by the shot peening operation are also shown in Fig. 2(A). This diagram also shows the dissipation of most of these stresses when the torsion bar was subsequently pre-set by overloading.

As previously explained (Refs. 1 and 3), adequate shot peening induces biaxial residual compressive stress ap-

proximating one half of the nominal yield stress of the peened metal. The nominal yield stress of steel having a hardness of Rockwell C-49-50 may be assumed to exceed 200,000 psi, from which the biaxial (compression-compression) peening stress induced in the torsion bar is assumed to be slightly greater than 100,000 psi as indicated in Fig. 2(A) by the stress components OJ and $O'M$.

The nominal compressive and tensile stress components at the surface of the torsion bar from the prestressing overloads were 225,000 psi; but since these stresses were superimposed upon the residual biaxial compressive stress induced by shot peening, the total nominal stresses for the immediate purpose are assumed to be the algebraic sums of the residual and applied stresses. The combined nominal stress in the direction of the compressive component of the torsional stress is therefore

$$OJ + ON_c = OJ'$$

Since this sum exceeds the yield stress of the metal by the amount Y_cJ', it is seen from this observation that all of the peening stress in the direction of the compressive component is immediately lost.

The combined nominal stress in the direction of the tensile component is

$$O'N_t - O'M = O'M'$$

In this direction, the portion Y_tM' of the peening stress remains, but the greater portion N_tY_t was dissipated by plastic yielding.

Tensile Yielding Reduced

One effect of shot pending on the vulnerable surface layer was to reduce plastic yielding in the direction of the tensile component by the amount N_tM' and to increase plastic yielding in the direction of the compressive component by the amount N_cJ'. It is not known whether the damage caused by extensive plastic yielding was reduced by this exchange or if the increased fatigue durability (shown in Fig. 17, p 179, Ref. 4) resulted solely from decreasing the magnitude of the applied stress in the direction of the tensile component.

After release of the prestressing load, the two residual stress components in the bar were as indicated by the broken line $DEFGG'$ in Fig. 2(B). It is seen that the residual stress $O''FGG'$, in the direction of the nominal tensile component of this diagram, is identical with $O''FGG'$ of the torsional diagram Fig. 1 including the remnant GG' of the peening stress. The residual stress DEO'' in the direction of the nominal compressive component of Fig. 2(B) is also like the diagram Fig. 1, except that it is inverted and no portion of the peening stress remains.

Tensile Component Reduced

The maximum load that was applied during the fatigue test stressed the torsion bar to a nominal value of 145,000 psi, as is indicated by the diagonal dash line $N'_tN'_c$, Fig. 2(B). The maximum stresses were the algebraic sum of these nominal applied stresses and the residual stresses, as indicated by the broken line $K'KH$. It is seen that the combined effect of prestressing by overload and by shot peening reduced the tensile component of the applied stress by the amount N'_tK'. The surface tensile component, which because of surface weakness (Ref. 2) is the direct cause of fatigue failures in specimens that are not adequately prestressed, was thus reduced from 145,000 to approximately 113,000 psi.

The diagram Fig. 2(C) indicates the stress range that was applied during the fatigue test as modified by the residual stresses from the nominal unidirectional range of 20,000 to 145,000 psi. It is seen that, in approximate terms, the surface compressive component $D'H$ ranges from 2,000 psi compression to 127,000 psi compression, and that the surface tensile component $K'G''$ ranges from 113,000 psi tension to 12,000 psi compression.

This method, as used in the preceding paragraphs for combining the biaxial residual compressive stress from shot peening and the biaxial torsional stress from the prestressing overload, is an oversimplification that leads to errors in the resultant stress magnitudes. Although these quantitative errors are undesirable, it is believed that the diagrams of Fig. 2 correctly represent the qualitative effects.

Combining Biaxial Stresses

A more accurate method for combining such biaxial stresses has been developed by Mr. Robert Schilling of the Research Laboratories Division, General Motors Corporation. This method, which makes use of the conventional yield ellipse, is being prepared for early public presentation.

The Schilling method will indicate that less plastic yielding occurred from combining the peening and pre-setting stresses than is shown in Fig. 2(A). It will also indicate that a small peening residual stress was retained in the direction of the compressive component (upper part of diagram) as well as a greater stress in the direction of the tensile component (lower part of diagram). The retaining peening stress components were, of course, unequal in magnitude else no peening stress would have been detected by the dissection stress analyses.

The net effect of the Schilling method is expected to be that the (harmful) surface tensile stress is reduced by a greater quantity than KK' as is indicated in Fig. 2(C) with corresponding increases in the compressive stresses of the same diagram. Since this latter increase is in the elastic range, it does not affect the fatigue strength of the specimen.

Prestressing at High Temperature

It is probable that the greater part of fatigue damage from extensive plastic yielding could have been avoided by performing the prestressing operation at an elevated or higher temperature.

The production tempering specification required a ". . . minimum time at heat of two hours at not less than 850 F to produce hardness of . . . 47-51 Rockwell C." Presumably, therefore, prestressing could have been performed at a temperature where the bars were more ductile and plastic flow could occur with relatively less fatigue.

This precaution was observed in straightening the bars after heat-treatment. According to specifications, the straightening operation was performed " . . . from draw heat at a temperature of not less than 600 F." Even at this temperature, straightening by applying a bending load could be extremely damaging to those hard torsion bars, because the process induced residual tensile stress on one side of the bar and required yielding by direct tension on the opposite side. Direct tensile yielding could, and probably did, develop transverse cracks in bars that required extensive straightening.

A number of experimental bars were given a second shot peening after pre-setting, which presumably increased surface residual compressive stress but it also required additional plastic flow. Tests of these doubly shot peened bars did not show greater fatigue life than resulted from a single peening prior to pre-setting. In one case the double treatment indicated a loss in fatigue strength, which is a relatively common experience with overpeened parts, but it is more probable that the loss in fatigue strength was due to defective material than to overpeening.

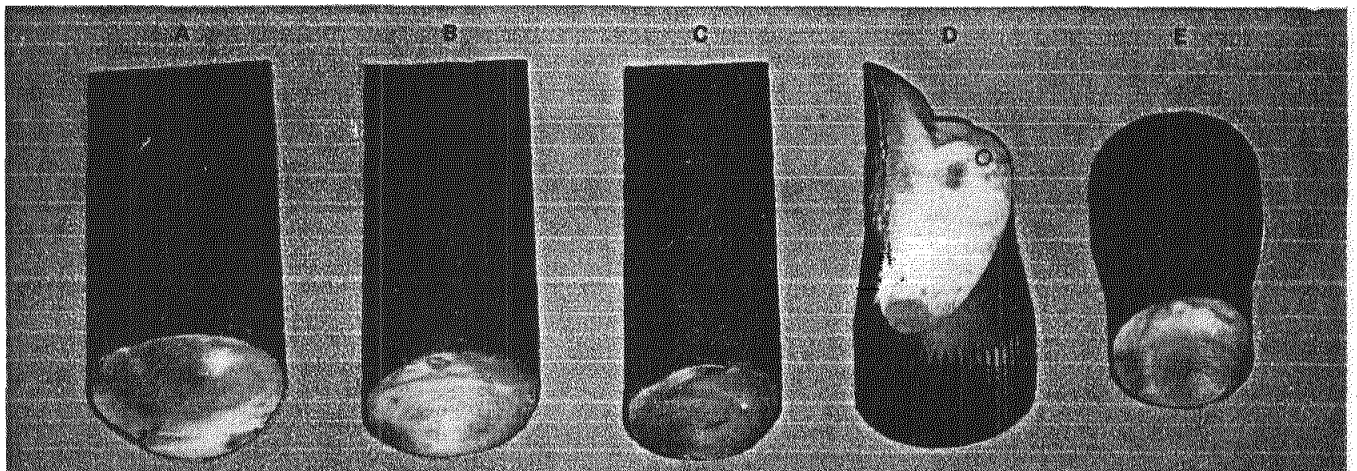

Fig. 4—Decarburization and consequent extensive plastic yielding during unidirectional-fatigue tests caused shear failures in four of five bars.

Table I—Yield and Fracture of Torsion Bar Specimens

Torsion Bar	Decarb. Depth, in.	Core Hardness, RC	Cycles Failure	Yield, in.			Longitudinal Defects	Character of Fracture
				5,000 Cycles	10,000 Cycles	20,000 Cycles		
A			43,000	0.835			Short	Shear
B			29,000	0.793			Short	Shear
C			30,000	0.665		0.96	Short	Shear
D	0.009	47	40,000	0.710	0.72		Short and long	Tension
E	0.018	47	25,000	0.751		0.84	Short	Shear

Processing Variations Reveal Valuable Data

As a result of numerous experimental variations in processing of military vehicle torsion bars and because the effect of each variation was measured by many fatigue tests, valuable data bearing on the characteristics of torsional failures are available. Among these are transverse and longitudinal fractures that tend to confuse the observer as to causes of fatigue and the remedial measures that may be applied.

The characteristics of fractures that developed in five experimental torsion bars from applying repeated unidirectional twisting loads ranging from 38,000 to 137,000 psi are shown in Fig. 4. These bars differed from regular production bars in a number of details. From the standpoint of fracture characteristics, the most important differences were that their surfaces were in the rough 'as rolled' condition presumably in the interest of lower cost, and pre-setting was omitted presumably as a step in measuring the value of residual stress induced by this operation.

Bars A, B, C, and E shown in Fig. 4 are seen to have failed by transverse shear, only bar D failed by tension in the manner that would be expected. Transverse failures occurred in most of the specimens because the applied load stressed the bars above their yield strengths and extensive plastic yielding continued throughout each test.

Although the maximum nominal test stresses were somewhat lower than were applied to standard production bars (such as is shown in Fig. 16 Ref. 4) their elastic strengths were exceeded because their unfinished surfaces were decarburized. The decarburized layers were incapable of sustaining their share of the applied loads (Ref. 2), therefore, the stresses in the underlying metal were increased sufficiently to cause extensive plastic creep. The compressive and tensile stress components contributed in substantially equal amounts to the plastic deformation, therefore, after a sufficient number of stress applications the failures resulted from the combined effects of these components to exhaust the capacity of the steel to plastic flow. These specimens are seen to have behaved in the same manner as the modeling clay cylinder shown in Fig. 2(B) of Sept. 1951 article.

The depth of decarburization and subsurface hardness were measured in bars D and E as shown in Table I. In terms of the standing height of the vehicle, Table I also records the extent of plastic yielding of all bars in the group after 5,000, of one bar after 10,000, and of two bars after 20,000 load applications.

A punch press, operated at constant stroke, was used as the fatigue machine. Because plastic yielding continued throughout the tests the applied stress necessarily decreased between periods of load adjustment. Since load restorations were made only after 100, 500, 1,000, 5,000, 10,000, and 20,000 cycles, the average applied stress varied appreciably below that of the specified load.

Magnetic particle inspection, which was applied to each of the five torsion bars prior to fatigue testing, revealed short longitudinal seams in all bars as noted in Table I. In only one

specimen, bar D, was the character of the fracture dominated by these defects. This bar had, in addition to several short defects, a 5 in. seam near the end of the bar. This long seam acted as a stress raiser for the development of a normal tensile fatigue fracture, the origin of which is indicated in Fig. 4 by a circle. It is probable that, as noted in Table I, the smaller depth of decarburization in bar D was responsible for its greater fatigue durability and its relatively low plastic settling.

Good Reports Require Good Photographs

Photographic records of the fatigue fractures of the subject torsion bars were superior to those usually found in routine laboratory reports, but in only ocasional instances are they adequate for diagnostic purposes. A selected few show sufficient detail to establish definitely the point at which fracture originated and to identify material defects that caused or contributed to the failure. Note, for example the inadequacy of the photograph of bar D of Fig. 4. The report relating to this specimen states that the fracture developed from a longitudinal defect. The point at which the fracture originated can be discerned in the photograph but, because of the angle at which it was taken, no evidence of the defect is seen.

Similarly located fatigue fractures from the same causes are better illustrated in specimens F and G, Fig. 5. These bars differed from the bars shown in Fig. 4 in that their surfaces had been machined to remove decarburized metal and they were also otherwise processed to standard specifications, including prestressing. The bar F was tested at a nominal stress range of 8,500 to 135,500 psi and failed after 87,000 stress cycles. The bar G was tested at a nominal stress range of 22,500 to 150,000 psi and failed after 47,000 stress cycles.

The excellent photographs of bars F and G, Fig. 5, clearly show the points of origin of fatigue fractures as well as the open seams that served as stress raisers to hasten failure. Note that the longitudinal planes of the seams are discolored by heat-treatment and that they are entirely free of characteristic fatigue marking. In both specimens, fractures originate at the junction of the longitudinal fissure and the outer surfaces of the bars. It is also seen that the fatigue fractures advanced from their points of origin at angles of approximately 45 deg to the axes of the bars, that is, the fractures are normal to the tensile components of clockwise torsional loads.

Other details of the fracture surfaces are relatively unimportant because the states of stress in the remaining sections were drastically altered by the advancing fractures. Such unimportant features, however, are often found described in detail and no mention made of the important characteristics. In other instances, clearly defined evidence pointing to the fracture origin and to the contributing causes of fracture is interpreted erroneously.

The metallurgist's report on the fatigue fracture of bar I shown in Fig. 6 states that the fracture originated in the longitudinal defect that appears on the lower edge of the fracture. When discovered by magnetic particle inspection before fatigue testing, this defect was found to be 3.5 in. long. Probably because of prior knowledge of the presence of this defect and because evidence of it appeared in the fracture, the unwarranted conclusion was reached that this defect was the origin of fatigue failure, notwithstanding the well defined nucleus a short distance below the opposite surface of the bar. From the same bar, the section H in Fig. 6 was removed a short distance from the fracture to show another longitudinal seam, this one 2 in. long.

Principal interest in the fracture of bar I, Fig. 6, is that: (1) Its point of origin was not influenced by the presence of at least two major longitudinal defects; (2) the fracture was caused by the tensile components of counter clockwise torsional loads; and (3) the point of greatest effective stress was approximately 0.35 in. below the surface of the bar. Direct evidence is not available, but it is probable that a large inclusion or similar defect served to amplify the stress at the fracture origin.

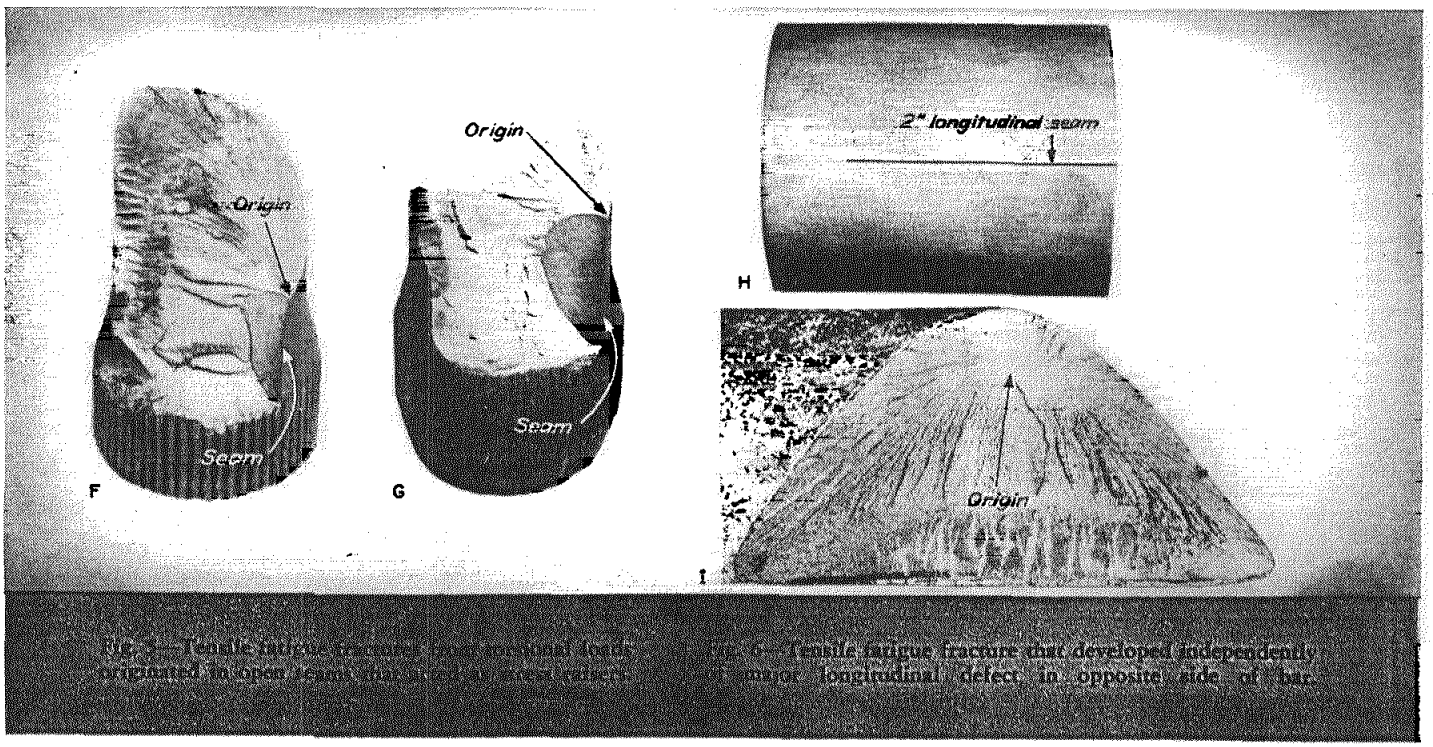

Fig. 5—Tensile fatigue fractures from torsional loads originated in open seams that served as stress raisers.

Fig. 6—Tensile fatigue fracture that developed independently of major longitudinal defect in opposite side of bar.

Extra Hard Torsion Bars

The fractured specimens L and M of Fig. 7, which failed by tension from repeated clockwise twisting loads, are also of sub-surface origin but their nuclei are not so deep as the nucleus in Fig. 6. No effort seems to have been made to determine the nature of the stress raisers that contributed to these failures. But since the nuclei were between 0.1 and 0.2 in. below the surface, where the nominal prestressing stress was 85 to 90 percent of the nominal surface stress, possible damage during prestressing should be suspected as well as defects originally present in the material.

These specimens were made to standard specifications except in hardness. They were tempered at 750 F to Rockwell C 54, whereas standard production bars were tempered at 850 F to Rockwell C 49. These specimens were therefore more susceptible to damage from plastic yielding during prestressing and to early failure from this damage than bars tempered to greater ductility.

Because fatigue weakness of surfaces increases with brittleness, compressive stresses induced by shot peening and other superficial mechanical operations become more effective in increasing fatigue strength as hardness of the peened steel is increased. Since surface weakness, however, is relatively just as detrimental to the internal surfaces of defects such as inclusions, voids, seams and cracks, as to external surfaces, and since these internal surfaces cannot be reached by peening through hardened highly stressed machine parts must be as free of internal defects as possible.

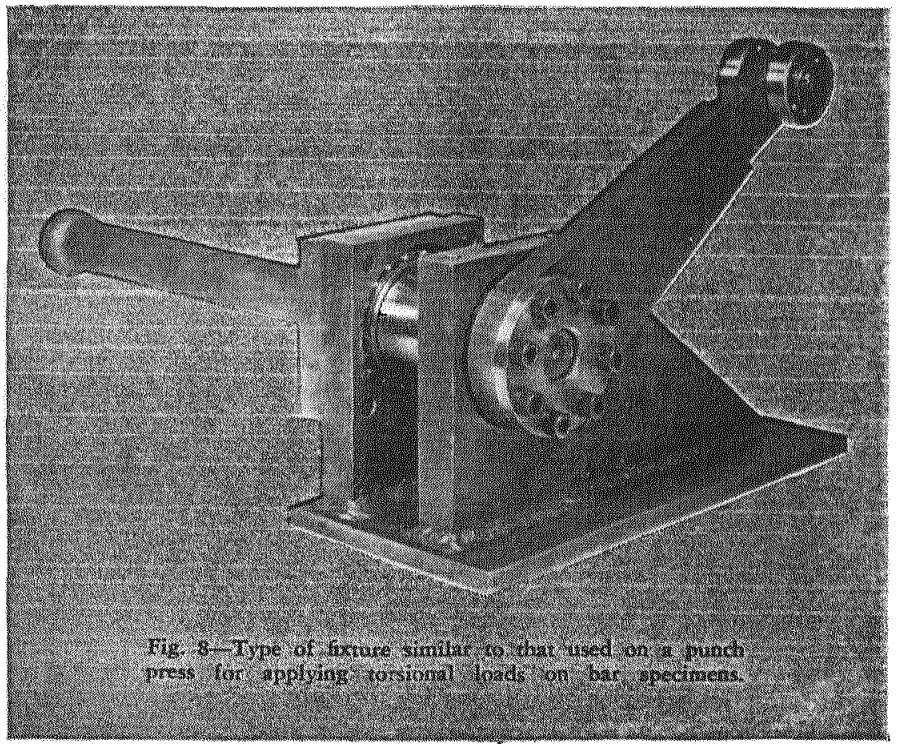

Fig. 8—Type of fixture similar to that used on a punch press for applying torsional loads on bar specimens.

Deep Prestressing

Prestressing by overloading is the only mechanical process now in use that is capable of inducing favorable residual stresses at depths sufficient to be effective against defective steel. Even this operation is relatively ineffective against any deep defect in very hard steel unless damage from extensive plastic yielding is reduced by prestressing at an elevated temperature.

Torsion bars L and M, Fig. 7, failed after 66 and 310 load applications respectively while being fatigue tested at nominal stresses ranging from 8,500 to 135,500 psi.

The fatigue fracture of torsion bar K, Fig. 7, also originated in sub-surface metal but in this case the stress raisers that hastened failure are prominent in the photograph. This specimen was not only afflicted with a longitudinal seam but a transverse defect is also in evidence. Characteristic fatigue markings have their origins at the junction of the 45 deg plane of the tensile fatigue fracture with the 90 and 0 deg planes of the two defects.

This longitudinal seam, like the same defects in other specimens, was no doubt formed during rolling of the bars at the steel mill. The transverse defect could be, and probably was, a result of straightening after heat-treatment. The original report does not venture an explanation.

The bar was made to standard specifications except that it was given a second shot peening after pre-setting. Additional peening could not, however, have affected its fatigue strength because the origin of the failure, being sub-surface, was out of reach of the shot.

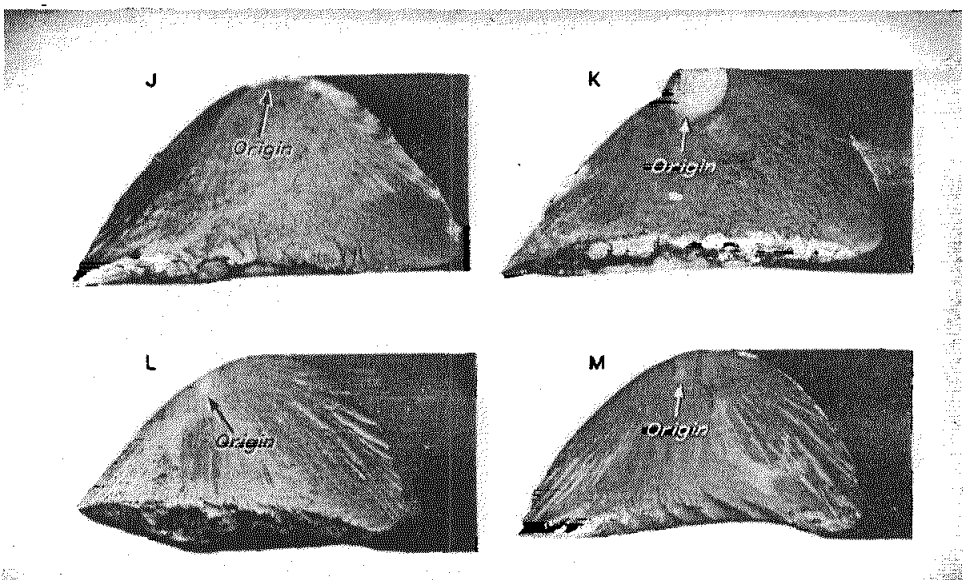

Fig. 7—Tensile fatigue fractures in extra hard torsion bars. Specimens failed under torsional loads. These failures originated in various sub-surface defects.

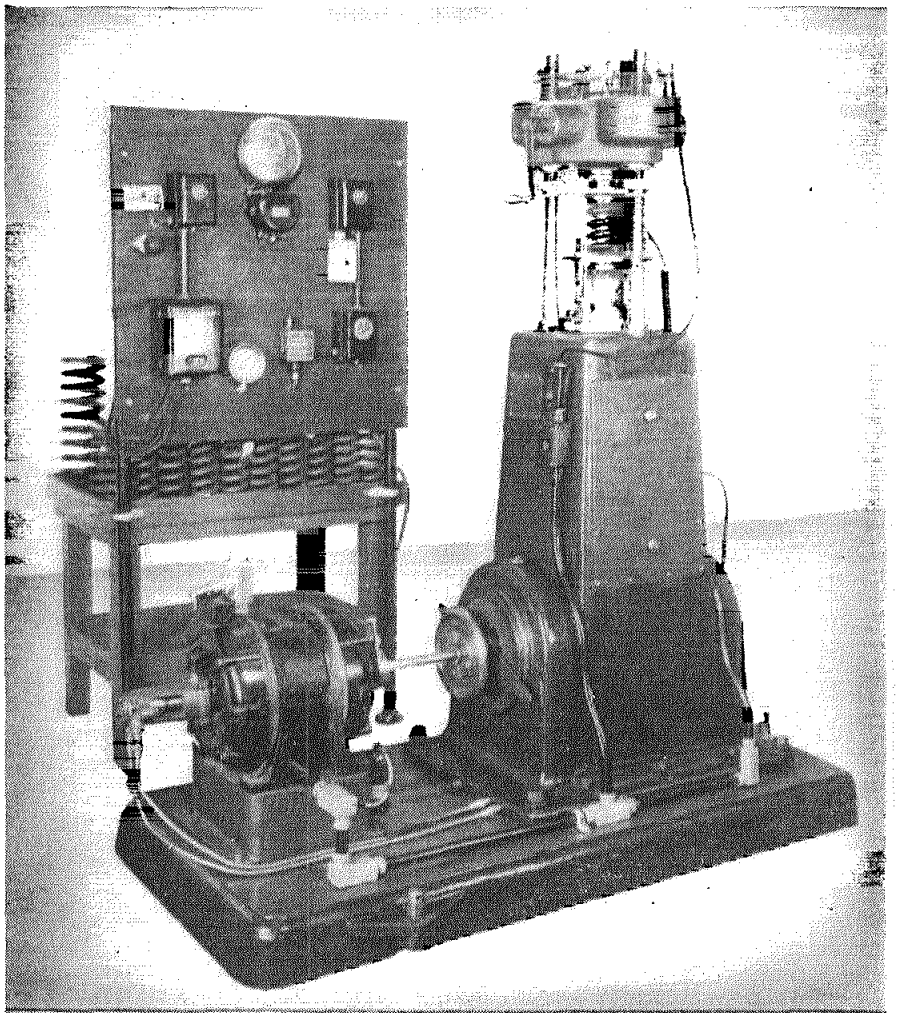

Fig. 9—Resonance type spring testing machine having a set speed of 1,200 cycles per second. As here shown, the coil spring mounted in the head of the machine is under test to determine fatigue life. A special fixture for loading bars in torsion can be installed in machine head.

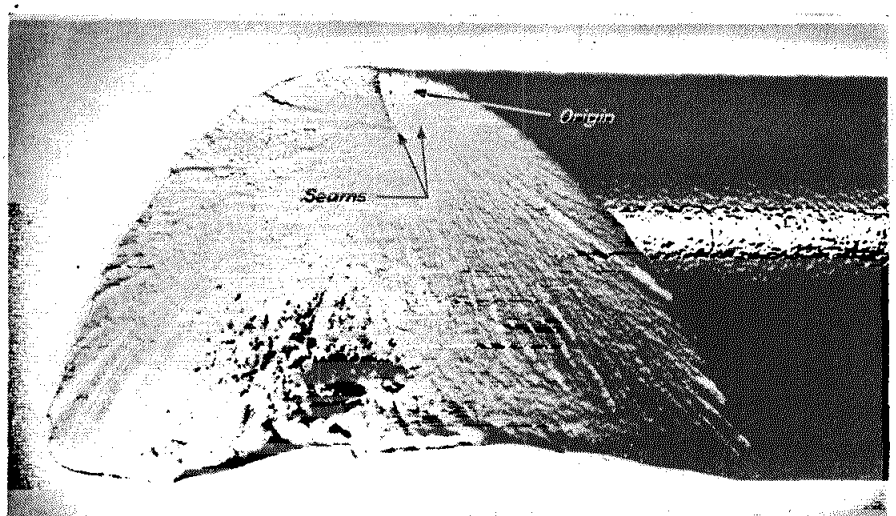

Fig. 10—Tensile fatigue failure from repeated clockwise torsion loads has its origin below surface between short seams. Processing included shot peening followed by prestressing.

Considering the severity of the stress raisers the durability of the specimen was good. It failed after 81,400 cycles at nominal stress ranging from 8,500 to 135,500 psi.

The original report on the specimen J, Fig. 7, states that the failure is of sub-surface origin, but the photograph does not show details beyond the fact that the fracture advanced at a 45 deg angle to the bar axis and downward from the top. This bar failed after 23,600 cycles at the same nominal stress range as was applied to the three specimens K, L and M. Its short life supports the original statement that failure originated below the surface, presumably in a relatively large defect.

Photographic Details Important

The photograph Fig. 10, showing the fatigue fractured section of one of a group of four torsion springs, is so sharp in all details that the point of fracture origin is clearly seen to be a short distance (0.04 in.) below the upper surface between two short longitudinal seams. Crack width was confined to the narrow space (0.13 in.) between the two seams until its inward growth on a 45 deg plane exceeded the depth of the seams (0.22 in.) after which it spread in all directions.

This bar was made from X-9165 steel heat-treated to a hardness in the range of Rockwell C 47-49. Processing included shot peening followed by prestressing. Examination indicated the presence of longitudinal defects with nonmetallic inclusions in all bars of the group. The bar illustrated was fatigue tested by applying unidirectional loads at nominal stress ranging from zero to 137,000 psi. Failure occurred after 30,000 stress applications.

Torsional Fatigue Failures Are Tensile Failures

Military vehicle torsion spring fatigue fractures have been discussed at considerable length because they show that, in spite of inherent planes of weakness, torsional fatigue failures are caused by and develop normal to the tensile component of the applied stress.

REFERENCES

1. J. O. Almen—"Fatigue Weakness of Surfaces", *PRODUCT ENGINEERING*, November 1950, p. 117.

2. J. O. Almen—"Fatigue Failures Are Tensile Failures", *PRODUCT ENGINEERING*, March 1951, p. 101.

3. J. O. Almen—Kent's "Mechanical Engineers Handbook", Twelfth edition, Design and Production Volume, p. 20-40 to 20-48 inc.

4. J. O. Almen—"Torsional Fatigue Failures", *PRODUCT ENGINEERING*, September 1951, p. 167.